The human chorion contains definitive hematopoietic stem cells from the 15th week of gestation

Marcus O. Muench[1,2,3], Mirhan Kapidzic[3,4,5], Matthew Gormley[4,5], Alan G. Gutierrez[4,5], Kathryn L. Ponder[4,6], Marina E. Fomin[1], Ashley I. Beyer[1], Haley Stolp[4,5], Zhongxia Qi[7], Susan J. Fisher[4,5] and Alicia Bárcena[4,5]

[1]Blood Systems Research Institute, San Francisco, CA 94118, USA
[2]Department of Laboratory Medicine, University of California, San Francisco, CA 94143, USA
[3]These authors equally contributed to this project
[4]The Ely and Edythe Broad Center of Regeneration Medicine and Stem Cell Research, University of California, San Francisco, CA 94143, USA
[5]Center of Reproductive Sciences, Department of Obstetrics, Gynecology & Reproductive Sciences, University of California, San Francisco CA 94143, USA
[6]Department of Pediatrics, University of California, San Francisco, CA 94143, USA
[7]Department of Laboratory Medicine, Clinical Cytogenetics Laboratory, University of California, San Francisco, CA 94107, USA

Corresponding author: Alicia Bárcena, Ph.D., The Ely and Edythe Broad Center of Regeneration Medicine and Stem Cell Research, Center of Reproductive Sciences, Department of Obstetrics, Gynecology & Reproductive Sciences, 35 Medical Center Way, RMB 902E, University of California, San Francisco CA 94143-0665, USA. Phone: 415-476-1092, FAX: 415-476-1635. Alicia.Barcena@ucsf.edu

Keywords: human hematopoietic stem cells, chorion, extraembryonic development, hematopoietic development

Summary Statement

Second trimester human chorion, a fetal membrane, contains definitive hematopoietic stem cells capable of engrafting adult immunodeficient mice.

Abstract

We examined the contribution of the fetal membranes, amnion and chorion, to human embryonic and fetal hematopoiesis. A population of cells displaying a hematopoietic progenitor phenotype ($CD34^{++/+}CD45^{low}$ cells) of fetal origin was present in the chorion at all gestational ages, associated with stromal cells or near blood vessels, but was absent in the amnion. Prior to 15 weeks of gestation, they lacked hematopoietic *in vivo* engraftment potential. Differences in the chemokine receptor and β1 integrin expression profiles of progenitors between the 1^{st} and 2^{nd} trimesters suggest that these cells had gestationally-regulated responses to homing signals and/or adhesion mechanisms that influenced their ability to colonize the stem cell niche. Definitive hematopoietic stem cells capable of multilineage and long-term reconstitution when transplanted in immunodeficient mice, were present in the chorion from 15-24 weeks' gestation, but were absent at term. The 2^{nd} trimester cells also engrafted secondary recipients in serial transplantation experiments. Thus, the human chorion contains functionally mature hematopoietic stem cells at mid-gestation.

Introduction

Mammalian development entails asynchronous growth of the embryo/fetus and extraembryonic structures, principally, the placenta and membranes. The placenta, which develops in advance of the embryo/fetus to support its growth, was shown to be a hematopoietic organ in mice (Gekas et al., 2005; Ottersbach and Dzierzak, 2005) and humans (Barcena et al., 2009; Barcena et al., 2011; Robin et al., 2009; Serikov et al., 2009). The placenta is comprised of highly vascularized tree-like chorionic villi that sprout from the chorionic plate (CP) (Figs. 1A and S1A). The villous surface is covered by trophoblasts. During most of the 1st trimester, the chorion is also covered with villi, which regress into a bilayer of cytotrophoblasts (CTBs) and stroma (, 1B) to form the smooth chorion (SC) that surrounds the embryo/fetus, as the amnionic cavity enlarges (Benirschke et al., 2006). We reasoned that the common developmental origin of the placenta and the chorion (Hamilton and Boyd, 1960) might entail the simultaneous existence of cells with hematopoietic potential in both sites.

The anatomy of the fetal membranes is depicted in Fig.1. The amnion, the inner layer, is the most proximal membrane to the embryo/fetus (Fig. 1A and B) and includes an epithelial monolayer. Beneath lies an avascular stromal layer (Luckett, 1975). The SC, the outer layer that lies adjacent to the decidual cells that line the uterus (Fig. 1A and B), is comprised of multiple layers of CTBs and a stroma that fuses with the amnion stroma in the mature fetal membrane (Bourne, 1962; Cross, 1998). The amniotic epithelium and CTBs are ectodermal derivatives; their stromata arise from the extraembryonic mesoderm. Initially, the chorion and amnion are physically separated and as the pregnancy progresses, the amnion is positioned closer to the chorion and the adjacent stromal layers fully fuse around 17-20 wks of gestation (Ilancheran et al., 2009), forming the mature structure of the amnion-chorion (Fig. 1B and S1D).

The mouse chorion contains myeloid and definitive erythroid progenitors prior to chorio-allantoic fusion and before establishment of the fetal circulation within the placenta, suggesting the *in situ* generation of hematopoietic progenitors (Zeigler et al., 2006). Previously, we reported the presence of $CD34^{++}CD45^{low}$ cells in whole human fetal membranes, but their niche and, more importantly, their functional status as hematopoietic precursors have not been established (Barcena et al., 2011). This population also resides in the chorionic villi of the placenta and contains HSCs (Barcena et al., 2011). Here we asked whether the comparable region of the human chorion (Fig. 1B; shaded dark blue) contains HSCs throughout gestation.

Results

Hematopoietic progenitors in the extraembryonic compartment are restricted to the chorion and chorionic villi. To determine the exact location of phenotypically defined hematopoietic precursors observed in the amniochorion (Barcena et al., 2011), we isolated cells from the amnion, the chorion and, as a control, the chorionic villi from the same placentas across gestation and analyzed for CD34 and CD45 expression. The different anatomical regions analyzed are depicted in Fig. S1. The 40 weeks (wks) of human pregnancy are often divided into trimesters: 1st trimester (0-13 wks), 2nd trimester (14-27 wks) and 3rd trimester (28-40 wks). The chorion samples contained both the SC as well as the CP, which was denuded of villi by manual dissection (Fig. S1A and B) and in those samples of amniochorion, the amnion was separated from the chorion (Fig. S1C and E). The three tissues analyzed from 1st semester samples were not subjected to any further processing after the enzymatic digestion of the tissues as described (Barcena et al., 2009), while 2nd and 3rd trimester tissues were further processed to obtain the light density fraction. Fig. 1C shows the absence of cells co-expressing CD34 and CD45 in the amnion. In contrast, hematopoietic progenitors CD34^{++}CD45^{low} cells were readily detected in the chorion and the chorionic villi at all gestational ages. The presence of CD34^{-}CD45^{+} mature cells was observed in all samples and their frequency increases over gestation (Fig. 1C). Most of these cells are Hoffbauer cells, CD14^{+} macrophages, which represent the most abundant mature hematopoietic cells in extraembryonic tissues (Barcena et al., 2009).

Immunolocalization of chorionic CD34^{+}CD45^{low} cells throughout gestation. To identify the hematopoietic niche in the chorion, we localized CD34^{+}CD45^{+} cells using immunofluorescence and confocal microscopy (Fig. 2). The sensitivity of immunofluorescence techniques does not allow high and low levels of CD34 expression to be distinguished, as done by FACS. Therefore, we searched for cells coexpressing CD34 and CD45. A similarly low frequency of chorionic hematopoietic progenitors observed by the FACS analyses (Fig. 1C) was also seen by immunolocalization. These cells resided primarily within the mesenchymal compartment (Fig. 2A). During early gestation, when villi are forming, clusters of CD34^{+}CD45^{+} cells were observed next to vimentin^{+} cells (Fig. 2B). Regardless of age, these cells were frequently found in close contact with vimentin^{+} mesenchymal cells in the CP (Fig. 2C and D). CD34^{+}CD45^{+} cells were also found in a predominant perivascular location in the SC (Fig. 2E and F), near vessels containing CD34^{+}CD45^{-} endothelial cells. In addition, the number of individual and clusters of CD34^{+}CD45^{+} cells significantly increased from 1st to 2nd trimester. In conclusion, CD34^{+}CD45^{+} cells were frequently found associated with vimentin^{+} stromal cells in

1st trimester chorion, as well as in 2nd trimester CP, and primarily positioned near or within the vasculature in 2nd trimester SC.

The frequency and number of $CD34^{++}CD45^{low}$ cells vary across gestation. Hematopoietic progenitors were quantified from 51 chorion samples of different gestational ages. We defined a gate that contained the population of $CD34^{++}CD45^{low}$ cells (Fig. 3A). Primitive hematopoietic progenitors and HSCs are known to display low levels of CD45 on their cell surface and to increase CD45 expression as they differentiate (Mayani et al., 1993). We found chorionic $CD34^{++}CD45^{low}$ cells present at low frequency throughout gestation (0.01-1.9%, *n*=51). The density of $CD34^{++}CD45^{low}$ cells, measured as the mean number of cells per gram of tissue, was highest at 5-8 wks of gestation (Fig. 3B). In the 1st trimester, they gradually diminished to ~10^4 cells/g and this density persisted for the rest of gestation. Although there was variability among samples, the total number of $CD34^{++}CD45^{low}$ cells in the chorion substantially increased towards term (Fig. 3C). The number of cells per tissue ranged from: 1st trimester (*n*=21), 12-58 x 10^3 cells; 2nd trimester (*n*=21), 1.0-21 x 10^4 cells and 3rd trimester (*n*=9), 0.8-15 x 10^5 cells. These data show that the density of $CD34^{++}CD45^{low}$ cells was highest in the 1st trimester, while the absolute numbers were highest at term. These findings are in line with our previous observations in chorionic villi of the placenta (Barcena et al., 2009).

$CD34^{++}CD45^{low}$ cells in the chorion have a similar phenotypic profile as the equivalent intraembryonic population. The antigenic profiles of the light-density chorion cells are shown in Fig. 4 (n=3). At mid-gestation, there are abundant $CD34^{-}CD45^{+}$ mature cells, mainly Hoffbauer cells, and $CD34^{-}CD45^{-}$ cells, mostly comprised of stromal cells (data not shown). Analysis of $CD34^{++}CD45^{low}$ cells (gated in Fig. 4A) showed they expressed little CD38 and CD133, low levels of CD117 and CD4, and medium to high levels of HLA-DR, CD31, CD90, CD95, Tie2 (CD202b, angiopoietin receptor 2) and CD71. These data suggest that the $CD34^{++}CD45^{low}$ population is heterogeneous, possibly including both hematopoietic and endothelial lineage ($Tie2^{+}$) cells (Fig. 4B). In addition, this population displayed variable levels of CD13, CD33, and EpoR (data not shown) and did not coexpress KDR (VEGFR2, CD309) or CD150 (Fig. 4B). Thus, the $CD34^{++}CD45^{low}$ cells in the chorion displayed a phenotypic profile similar to the most primitive subset ($CD38^{-/low}$) intraembryonic counterpart population from fetal liver and bone marrow (BM), and was very similar to placental hematopoietic progenitors (Barcena et al., 2009; Bárcena et al., 1996; Muench et al., 1997).

Transplantation of chorion cells into immunodeficient mice shows that they contained HSCs. First, we identified the dissociation method that yielded the maximum number of repopulating HSCs. Collagenase digestion of the chorion failed to release cells that engrafted

mice (Fig. 5A). Transplanted $CD34^{++}CD45^{low}$ cells and their mature progeny ($CD34^{-}CD45^{+}$ cells) were detected only after the chorion samples were subjected to serial enzymatic digestion by collagenase IA, followed by trypsin (Fig. 5A). The level of human cell engraftment in the BM obtained with cells isolated using collagenase IA and trypsin was similar in both mice (~23%). The gating strategy employed to determine the frequency of human cells is shown in Fig. S2A. Multilineage engraftment was observed in these mice, with 24-30% B cells ($CD19^{+}$ cells), 18-19% erythrocytes ($CD235a^{+}$ cells), 7-8% myeloid cells ($CD14^{+}$ and $CD66b^{+}$ cells), as well as 35-37% $CD34^{+}$ progenitor cells.

We investigated the hematopoietic engraftment potential of chorionic cells of different gestational ages. The vast difference in the number of cells that can be obtained from 1st vs. 2nd trimester chorion samples prevented us from cell-sorting specific populations (i.e., $CD34^{++}CD45^{low}$) across all gestational ages. In addition, the low frequency of $CD34^{++}CD45^{low}$ cells (0.01-1.9%) leads to very long cell sorts, which might affect cell purity and viability. Therefore, we transplanted unfractionated cell suspensions of enzymatically digested 1st trimester chorion samples and the light density fraction of samples older than 12 wks, which are enriched in $CD34^{+}$ cells. In addition, for 2nd trimester chorion samples (≥14 wks), lineage (lin-) depletion was performed, as described in Supplemental Methods. The transplanted cells were obtained by processing the entire CP and the SC together (2nd trimester) or 30-50 g of 3rd trimester tissues. Five to 10 mice were transplanted with each specimen with 1-27 x 10^5 cells/mouse (1st trimester), 0.1-22 x 10^5 cells/mouse (2nd trimester) and 2-6 x 10^5 cells/mouse (3rd trimester). Mice were analyzed from 9-30 weeks post-transplant, with the majority of analyses done between 100-150 days. It has been reported that 7-10 wks after transplant provides sufficient time to observe reconstitution derived from HSC (Goyama et al., 2015; McKenzie et al., 2007), while more mature progenitors ($CD38^{+}$) disappeared by 4 wks (Kerre et al., 2001). Mice transplanted with chorion cells <15 wks of gestation showed no multilineage engraftment (Fig. 5B). In two cases, limited reconstitution by mostly myeloid- and/or T-cells was observed in some or all of the mice (Fig. S3). With some variability, multilineage long-term hematopoietic reconstitution was detected from the 15th wk of gestation onward (Fig. 5B). A general absence of repopulating HSCs was observed from late pre-term (34 wks, 5 days) and term (38 to 39 wks) chorionic cells: only 1 out of 26 mice transplanted displayed full multilineage reconstitution, while 7 out of 26 mice had partial human engraftment (Fig. 5B). Our data showed that definitive HSCs were present in the chorion from 15 to 24 wks, while prior to 15 wks no HSC activity was detected, and during the 3rd trimester HSC were extremely rare. In Fig. S3 we provide more detail on the transplantation experiments summarized in Fig. 5B.

It is well established that HSCs occupy a hypoxic niche in the BM and that this environment maintains their repopulating potential and their quiescent state (Kubota et al., 2008). Accordingly, we performed CFU-C assays in hypoxic (1% O_2) and standard (20% O_2) conditions with four chorionic samples of 5-10 wks of gestation. We found that hematopoietic colony growth was not significantly affected by physiological hypoxia (Fig. S4A). Many non-hematopoietic colonies displaying fibroblast morphology were observed. The number of CFU-fibroblast obtained in hypoxic conditions was generally higher than in normoxic conditions (Fig. S4B). Based on these findings, we concluded that the lack of engraftment by early gestation samples was not simply explained by a requirement for a low O_2 environment.

Chorionic HSCs generate multilineage progeny in immunodeficient mice and can be serially transplanted. Multiparametric FACS analyses were performed on the BM, spleens and livers of animals engrafted with $CD59^+$ 2nd trimester lin^- chorion cells (22 wks) using previously detailed methods (Varga et al., 2010). Total BM samples were analyzed to ensure the detection of $CD235a^+$ erythrocytes, which were otherwise depleted during isolation of light-density cells from spleen and liver samples. At 148 days post-transplant, the median level of human cell engraftment in the BM was 21.6% and ranged between 4.5 and 58% (n=10). Human chimerism was higher among splenocytes, which contained a median of 82% human cells (range 30.4-93.7). Fig. 6 shows multilineage engraftment in a mouse with a high level of human chimerism. We used CD59 to identify all human cells, including mature $CD235a^+$ erythrocytes (Fig. S2B). $CD45^+$ leukocytes contained a substantial $CD34^+$ hematopoietic progenitor population. The human cells were at different stages of maturation, from HSCs ($CD34^{++}CD133^+$) and early progenitors ($CD34^{++/+}$) to intermediate progenitors of the B-cell ($CD34^+CD19^+$ cells), myeloid ($CD34^+CD33^+$ cells) and erythroid lineages ($CD34^+CD235a^+$). In addition, the BM of transplanted mice contained mature B cells ($CD34^-CD19^+$ cells), mature myeloid cells ($CD34^-CD45^+CD33^+$ cells), erythrocytes ($CD34^-CD235a^+$ cells), T cells ($CD3^+$ cells) and natural killer (NK) cells ($CD56^+CD3^-CD7^+$). In the spleen, we detected erythrocytes, monocytes ($CD14^+$ cells), platelets ($CD41^+CD42b^+$) and single positive $CD3^+CD4^+$ and $CD3^+$ $CD8^+$ T cells. $CD34^{++}CD133^+CD38^{-/low}$ were also observed in the liver, consistent with previously observations that the adult mouse liver supports this primitive population of hematopoietic precursors (Muench et al., 2014).

To further verify long-term reconstituting HSC engraftment, serial transplantation was performed in which the BM of primary recipients was transplanted into secondary recipients. Light density lin^- chorion cells from a 24 wk sample were transplanted into two primary recipients and their BM was harvested 68 days later. Multilineage engraftment was observed in the BM of both mice with frequencies of 43% or 53% human cells (data not shown). BM was

pooled for transplantation into secondary recipients, which each received the equivalent of 36% of the BM content of single femur. The BM of secondary recipients was analyzed after 92 days and contained 19-21% human cells (Fig. 7). The primitive progenitor population ($CD34^{++}CD133^{+}CD38^{-/low}$) was readily detected, as well as B cell progenitors, myeloid cells and erythrocytes. The myeloid population contained granulocytes ($CD33^{+}CD66b^{+}$) and monocytes ($CD33^{+}CD14^{+}$). In the spleen, platelets and T cells (single positive for CD4 or CD8) were present. These data demonstrate that the mid-gestation chorion contains HSCs capable of long-term, multilineage hematopoiesis with secondary transplant potential in adult hosts.

Extreme limiting dilution analysis (Albelda et al.) of chorion HSCs in immunodeficient mice. ELDA was performed to determine the frequency of HSCs among chorionic cells from two mid-gestation lin^{-} samples (20 wks) (Hu and Smyth, 2009). Phenotypic analyses of the chorion cells prior to transplant showed that the frequency of potential HSCs ($CD34^{++}CD45^{low}CD133^{+}$) was low (1-4 cells in $1x10^{3}$ of the light density, lin^{-} fraction; data not shown). The estimated frequency of engrafted HSCs was 1 in 3.3×10^{4} light-density lin^{-} cells in one experiment (Fig. 8A) and 1 in 8.2×10^{4} light-density lin^{-} cells in the other (Fig. 8B). Using these values, we calculated that the transplantation of 33-132 (experiment 1) or 82-328 $CD34^{++}CD45^{low}CD133^{+}$ cells (experiment 2) produced multilineage, long-term engraftment in mice. These frequencies are similar to those reported for human BM HSCs (Guezguez et al., 2013).

There is no universally agreed upon definition of engraftment used as an indicator of HSC activity in immunodeficient mice. We used a strict definition to define full engraftment (presence of three lineages) that included detection of $CD34^{+}$ cells as an indication of ongoing hematopoiesis, although failure to detect human red cells was often the cause of partial engraftment. Partial engraftment was detected in many mice in the limiting dilution analyses in a pattern consistent with the dose of cells transplanted (Fig. 8C and 8D). As some of these mice may have been engrafted with HSC but failed to achieve sufficient multilineage engraftment for detection, our estimate of HSC numbers may be low. In addition, the R values for the graphs shown in Fig. 8A and 8B were higher than 1, which implies that engraftment was hyper-responsive to dose. This behavior suggests multi-hit alternatives (Hu and Smyth, 2009), *i.e.*, the presence of more than one cell population cooperating to produce full human cell reconstitution in mice or the cooperative effects of human hematopoietic cells in supporting their own growth and differentiation.

Sorted CD34^{++}CD45^{low} chorion cells are of fetal origin and reconstitute immunodeficient mice. To determine the origin of HSCs residing in the chorion, we sorted CD34^{++}CD45^{low} cells from an 18.3 wks of gestation male CP+ SC whole chorion sample. Since the number of cells obtained was very low, we expanded them for 3.5 days *in vitro* in the presence of cytokines, after which we performed fluorescent *in situ* hybridization (FISH) with probes specific for the X- or Y-chromosomes. The results indicated that this population was of fetal origin, as 98% of the cells were male (Fig. 9A). Next we sorted CD34^{++}CD45^{low} cells from a male SC sample, 23.6 wks of gestation, and transplanted them into NSG-3GS mice (3 x 10^3 cells/mouse). After 61 days, multilineage human engraftment was observed in the BM, including erythroid, lymphoid (B-, T- and NK-cells) and myeloid cells (Fig. 9B). The spleen contained human platelets and T cells (Fig. 9C), while the liver contained a CD34^{++}CD133^{+} HSC population (Fig. 9D). The BM from all 4 of the transplanted mice showed full human reconstitution and they were pooled to sort CD34^{++}CD45^{low} cells. FISH analysis showed that 100% of these cells were male. Identical results were obtained on sorted CD34^{-}CD45^{+} cells, demonstrating that the mature hematopoietic cells generated in the transplanted mice are also of fetal origin (data not shown). From these results we concluded that the HSC potential of the chorion samples resides within the CD34^{++}CD45^{low} population and is not maternally derived.

Chemokine receptor and adhesion molecule expression of 1st and 2nd trimester CD34^{++}CD45^{low} chorion cells. We asked whether functional differences among chorion HSCs before and after 15 wks of gestation could be due to differential expression of chemokine receptors and adhesion molecules involved in homing to and retention in the mouse BM. We focused on chemokine receptors previously reported to be expressed by HSCs from human umbilical cord blood and BM (Aiuti et al., 1997; Basu and Broxmeyer, 2009; Broxmeyer et al., 2005; de Wynter et al., 1998; Levesque et al., 2003; Peled et al., 2000; Rosu-Myles et al., 2000; Su et al., 1997; Tarnowski et al., 2010; Torossian et al., 2014). First trimester CD34^{++}CD45^{low} chorion cells expressed low levels of CXCR7 and no detectable CD193 and CD195, but expression of the receptors increased in 2nd trimester samples (Fig. 10A). Conversely, we detected CD191/CCR1, which is expressed by CD34^{+} cells in the human BM (de Wynter et al., 1998; Su et al., 1997), only on 1st trimester CD34^{++}CD45^{low} cells. These data suggest that the developmentally regulated expression of chemokine receptors could be responsible for the functional deficits of early gestation chorionic HSCs. In this context, the expression of CCR1 alone failed to render functionally mature chorionic CD34^{++}CD45^{low} cells capable of

reconstitution. Instead, the cooperation among several chemokine pathways might be required for functional maturity in terms of homing.

Adhesion molecules are involved in HSC homeostasis, as they also regulate homing and retention of these cells to the BM niche. Thus, we asked whether chorionic $CD34^{++}CD45^{low}$ cells expressed adhesion molecules that play critical roles in these processes; specifically $\beta1$ integrins—$\alpha4\beta1$ (VLA-4, CD49d), $\alpha5\beta1$ (VLA-5, CD49e) and $\alpha6\beta1$ (VLA-6, CD49f)—as HSCs with repopulating capacity express these receptors (Imai et al., 2010; Notta et al., 2011; van der Loo et al., 1998). Fig. 10B shows high expression of CD49d and CD49e and medium levels of CD49f during the 1st trimester. In comparison, 2nd trimester chorionic $CD34^{++}CD45^{low}$ cells lacked CD49d expression, displayed similar levels of CD49e and increased levels of CD49f. The expression of other $\beta1$ integrins (CD49a [$\alpha_1\beta_1$], CD49b [$\alpha_2\beta_1$], CD49c [$\alpha_3\beta_1$]), also implicated in BM adhesion, were found to be present at similar levels regardless of gestational age (data not shown). Thus, the $CD34^{++}CD45^{low}$ cells isolated from the 1st and 2nd trimester chorion had different integrin expression profiles. Correlating these results with the *in vivo* transplantation data, suggested that the down regulation of CD49d and the up regulation of CD49f might be important signals for functional maturation of chorionic HSCs.

Discussion

Here we demonstrate the hematopoietic potential of the human chorion. It was previously reported that the mouse chorion possesses hematopoietic progenitors prior the establishment of fetal circulation (Zeigler et al., 2006) or the chorio-allantoic fusion (Corbel et al., 2007), thus pointing to the likely *in situ* generation of hematopoietic progenitors expressing *Runx1* and CD41. The notion that hematopoietic progenitors are engendered intrinsically in extraembryonic tissues was further supported by the finding of multilineage hematopoietic progenitors in mouse placenta of *Ncx1*$^{-/-}$ embryos, that lack heartbeat and, therefore, have no fetal blood circulation (Rhodes et al., 2008). These multipotent progenitors were able to produce erythroid, myeloid and lymphoid progeny *in vitro*. Although the self-renewing ability of mouse placental HSCs has been extensively documented (Gekas et al., 2005; Ottersbach and Dzierzak, 2005), the long-term repopulating activity of placental *Ncx1*$^{-/-}$ hematopoietic progenitors has not been addressed and whether the murine chorion contains HSCs remains unknown.

To our knowledge, this is the first demonstration of transplantable, definitive HSCs in the human chorion, which were absent in the amnion. Specifically, the chorion contained CD34^{++}CD45^{low} cells capable of long-term, multilineage reconstitution in mice and these cells could be serially transplanted into secondary recipients resulting in engraftment. By performing limiting dilution transplantation studies, we determined the estimated frequency of HSCs to be 1 in 3.3-8.2 x 10^4 light-density lin$^-$ cells. Taken all together our data demonstrated that the chorionic membrane provides an extraembryonic site of hematopoiesis during human gestation that harbors a resident population of HSCs, albeit at low frequency.

The primary goal of our study was to map the emergence and presence of hematopoietic precursors in the chorion during gestation. In line with our previously reported observations in placenta (Barcena et al., 2009), the early gestation chorion (5-8 wks) contained higher numbers of CD34^{++}CD45^{low} cells/g of tissue than observed later in development, although it is important to stress that this population of cells is always present at a low frequency (less than 1% of light density chorion cells). Their density significantly drops from the 9th wk onward, and is maintained at a constant level for the remainder of gestation. However, transplantation of early gestational age chorion samples occasionally produced one or two hematopoietic lineages (*e.g.*, unilineage T-cell reconstitution), but not multilineage engraftment in mice. In contrast, from the 15th wk of gestation onward, the chorion consistently contained definitive HSCs. This observation resonates with a report by Ivanovs *et al*., in which the authors reported transient unilineage T cells repopulation when transplanted early placentas (26-41 days of gestation) into

immunodeficient mice; multilineage, long-term engraftment was only accomplished when placentas 15-wks of gestation or older were transplanted (Ivanovs et al., 2011).

The mechanisms that orchestrate changes in the functional status of extraembryonic HSCs as gestation advances are not known. Cells with the phenotype of hematopoietic progenitors that were isolated from early gestation tissues may possess limited potential, and represent a primitive wave of hematopoietic progenitors unable to reconstitute mice. One potentially important player in the regulation of hematopoietic potential could be the hypoxic environment of extraembryonic tissues during early pregnancy. Since the placenta is not steadily perfused with maternal blood prior to 10-12 wks of pregnancy (Rodesch et al., 1992), physiological hypoxia could play a role in regulating hematopoiesis. It has been suggested that HSCs in the BM reside in a hypoxic niche that maintains their repopulating potential and their quiescent state (Kubota et al., 2008) and hematopoietic tissues in the mouse embryo—*e.g.*, the aorta-gonad-mesonephros (AGM) region, liver and placenta—are also hypoxic (Imanirad and Dzierzak, 2013). Likewise, the human chorion is poorly vascularized and possibly provides a hypoxic environment. We addressed the question whether the oxygen level could have a functional impact on early hematopoietic progenitors. Our data showed no consistent differences between CFU-C production at hypoxic vs. standard conditions. However, we could not rule out the possibility that hypoxia may work indirectly via the niche, which is dismantled when we isolate the cells.

An alternative explanation for the age-related functional disparities among chorionic hematopoietic precursors could be differences in their homing abilities and/or adhesion properties. We focused on receptors that are expressed by perinatal and postnatal HSCs. Our study shows that there are important differences among 1st and 2nd trimester chorionic CD34^{++}CD45^{low} cells with regards to their chemokine receptor expression profile. CD184/CXCR4, the CXCL12 receptor, plays a crucial role in regulating HSCs homing to the BM (Aiuti et al., 1997; Broxmeyer et al., 2005; Levesque et al., 2003; Peled et al., 2000). CD195/CCR5 ligands (CCL3, CCL4 and CCL5) modulate the chemotaxis of CD34^{+} cells in cord blood via the CD184-CXCL12 pathway (Basu and Broxmeyer, 2009). CD195 is expressed at higher levels on cord blood HSCs vs. those obtained from BM or mobilized to peripheral blood (Rosu-Myles et al., 2000). CXCR7, another CXCL12 receptor (Tarnowski et al., 2010), cooperates with CD184/CXCR4 in enhancing the effects of CXCL12 on cell cycling, survival and proliferation of CD34^{+} cells from peripheral blood (Torossian et al., 2014). In addition, CD34^{+} cells from umbilical cord blood express CD193 (Lamkhioued et al., 2003) and CD191 expression by CD34^{+} cells in cord blood confers superior engraftment of immunodeficient mice (de Wynter

et al., 2001). Our data showed that 1st trimester chorionic progenitor cells express CD191 (CCR1) and low levels of CXCR7, features that do not render transplantable chorionic $CD34^{++}CD45^{low}$ cells. Second trimester $CD34^{++}CD45^{low}$ cells, while were largely $CD191^{-}$, consistently expressed CD184, CD193, CD195 and CXCR7. Therefore, transplantable 2nd trimester chorionic HSCs shared the chemokine receptor profile with HSCs from perinatal and postnatal origins.

Similarly, 2nd trimester chorionic $CD34^{++}CD45^{low}$ cells share many characteristics with fetal liver and fetal BM HSCs/progenitors (expression of CD133, CD117, CD4, HLA-DR, CD95 – Fig. 4-, and CD13, CD33 –data not shown-). Despite the commonalities, definitive chorionic $CD34^{++}CD45^{low}$ cells display unique phenotypic properties, such as a predominant low level CD38 expression and their β1 integrin expression profile ($CD49d^{-}CD49e^{++}CD49f^{++}$). Second trimester fetal liver $CD34^{++}CD45^{low}$ cells coexpress CD49d (data not shown) and contain transplantable HSCs (Muench et al., 2014). Therefore, CD49d expression did not correlate with functional HSCs in the chorion. We conclude that the adhesion and homing properties of the extraembryonic niche might be different than the intraembryonic counterpart.

The origin of human extraembryonic HSCs is uncertain. Here we employed a FISH approach on 2nd trimester male chorion sample to establish the fetal origin of sorted $CD34^{++}CD45^{low}$ cells as well as their progeny produced *in vivo*. Despite their fetal origin, they could arise *in situ* to later populate the embryo/fetus. Alternatively, they might have an intraembryonic origin, colonizing extraembryonic structures once blood circulates. We cannot obtain chorion prior to 5 wks of gestation, therefore in all of our samples, the fetal-placental circulation was already established (Hamilton and Boyd, 1970). The AGM of 32-day-old human embryos (Carnegie stage 14) contains transplantable HSCs, preceding yolk sac, liver and placenta production of these cells (Ivanovs et al., 2011). Although suggestive, definitive proof that AGM-derived or liver-derived HSCs migrate to the placenta/chorion is lacking. Regardless, these extraembryonic structures could be sites of HSC generation. Our immunolocalization studies showed that the majority of the chorionic $CD34^{++}CD45^{low}$ cells were embedded within $vimentin^{+}$ stromal cells rather than associated with blood vessels, suggesting their possible origin from mesodermal progenitors in the stroma, which is derived from the extraembryonic mesoderm. This finding is in line with data from timed rescue of *Runx1* null mouse embryos, which showed that definitive, adult-type HSCs originate in the nascent extraembryonic mesoderm before the fetal liver initiates definitive hematopoiesis (Tanaka et al., 2012). We conclude that two separate hematopoietic niches coexist in the chorion: a predominant mesenchymal niche and a less common perivascular niche. The functional relationship between

these two hematopoietic niches or whether cells traffic between these locations remains to be determined. It would be very interesting to define, at a molecular level, the similarities and differences between the niches, which could lend functional insights into the regulatory networks of these two locations.

Materials and Methods

Isolation of hematopoietic progenitors from the amnion, chorion and placenta. Human tissues were obtained anonymously with the approval of the University of California, San Francisco Committee on Human Research. All donors gave written informed consent. Samples from 5-24 wks of gestation were from elective pregnancy terminations at San Francisco General Hospital. Full-term specimens collected at the time of delivery were from Moffitt-Long Hospital, University of California, San Francisco. The gestational ages of 1st trimester specimens were estimated based on crown-rump lengths, measured by ultrasonography. The gestational ages of 2nd trimester specimens were estimated by foot-length. The ages are expressed in weeks and days (i.e, 20.5 wks means 20 wks, 5 days).

Hematopoietic cells from chorion and amnion (separated from one another by manual dissection) were isolated as previously described (Barcena et al., 2009). Age-group specific tissue processing can be found in detail in Supplemental Methods.

Flow cytometry. Freshly isolated single cell suspensions were stained with mAbs (see Supplementary Table S1) and analyzed using a two-laser FACSCalibur or 3-laser LSR II cytometer (BD Biosciences). CellQuest (BD Biosciences) or FlowJo, version 9.2 (FlowJo, Inc., Ashland, OR) software was employed for analyses, which focused on live cells using an electronic gate to identify propidium iodide $(PI)^-$ events.

Human hematopoietic engraftment of mice. The animal studies were performed with the approval of the Institutional Animal Care and Use Committee at PMI Preclinical (San Carlos, CA, USA). Mice received humane care according to the criteria outlined by the National Academy of Sciences in the "Guide for the Care and Use of Laboratory Animals" and detailed in Varga et al. (Varga et al., 2010). Founder NOD.Cg-*Prkdc*^{scid} *Il2rg*^{tm1Wjl}/SzJ (NSG) and NOD.Cg-*Prkdc*^{scid} *Il2rg*^{tm1Wj}*I* Tg(CMV-IL3,CSF2,KITLG)1Eav/MloySzJ (NSG-3GS) mice, obtained from Jackson Laboratories (Sacramento, CA, USA) were maintained, bred and transplanted in a restricted access, specific-pathogen free vivarium at Blood Systems Research Institute, San Francisco, CA, USA. For additional details on the transplantation of human cells into mice as well as the harvest the mice tissues for engraftment analyses, please see Supplemental Methods.

Human chimerism in mice was studied between 63 and 214 days post-transplant; the majority of analyses were done between 100 and 150 days. Mice were sacrificed by carbon dioxide asphyxiation followed by cervical dislocation. BM was harvested by using a syringe with a 27-gauge needle to flush the femurs with approximately 3 ml of culture medium. Spleen and liver specimens were held in culture medium on ice until cell isolation. At the conclusion of the

experiment, mice were examined for signs of poor health or pathologies such as tumors of the liver, spleen, and/or thymus. Any moribund animals were removed from the study. Mouse BM, spleen and liver were processed as previously described (Varga et al., 2010).

The frequency of live human cells in the transplanted mice was determined based on the percentage of $CD59^+$ cells that lacked the expression of mouse markers (Fig. S2). The presence of transplanted HSCs was determined by measuring engraftment of myeloid ($CD33^+$, $CD14^+$, CD66b and/or $CD15^+$ cells), erythroid ($CD235a^+$), lymphoid ($CD19^+$ B-cells, $CD3^+$ T-cells, and $CD56^+CD3^-$ NK-cells) and hematopoietic precursor ($CD34^+$ $CD133^+CD38^-$ cells) cells by FACS. Engraftment of experimental mice was defined as a higher frequency of lineage marker-positive events in recipients as compared to control cells from an untransplanted mouse that were processed in parallel. Engraftment was defined as a minimum of 5 positive events above untransplanted controls. Full engraftment was defined as detection of all 4 cell types: myeloid, erythroid, lymphoid and precursors. Partial engraftment was defined as any engraftment less than full engraftment.

Hematopoietic progenitor assays. To enumerate CFU-Cs, methylcellulose clonal cultures of chorion cell suspensions were plated at a density of 2×10^3/35-mm plate (BD Falcon, BD Biosciences) in Methocult GF H4435 (StemCell Technologies, Inc., Vancouver, BC, Canada). Colonies containing myeloid cells or CFU-GM (CFU- granulocyte-macrophage progenitors) and CFU-mix (CFU-granulocyte-macrophage and erythroid cells) were scored after growth for 3.5 wks at 37°C in standard (20% O_2) or physiologically hypoxic (1% O_2) conditions.

Statistical Analysis of the data. For the estimation of HSC frequency in the mid-gestation chorion, ELDA (Albelda et al.) was performed according to the method of Hu and Smyth (Hu and Smyth, 2009). We employed ELDA software (http://bioinf.wehi.edu.au/software/elda/) to graph the results, which are also shown as box and whisker plots; median chimerism levels are indicated by a notch in the box.

Immunolocalization and fluorescence microscopy. Chorion tissue sections (20 μm) were fresh-fixed in 4% paraformaldehyde for 90 min and processed as previously described (Prakobphol et al., 2006). The tissue sections were stained with mAbs against CD34 (directly conjugated to FITC; clone 581, IgG_1, BD Pharmingen), CD45 (clones 2B11 + PD7/26, IgG_1, Dako, Glostrup, Denmark) and vimentin (clone SP20, Abcam Inc., Cambridge, MA,). For controls and secondary antibodies, please see Supplementary Methods. Staining with DAPI in Vectashield mounting medium (Vector Laboratories, Burlingame, CA) was used to visualize nuclei. Slides were imaged on a Leica DM 6000-CS microscope integrated with the Leica TCS SP5 confocal platform (Leica Microsystems, Inc., Buffalo Grove, IL).

Cell sorting of $CD34^{++}CD45^{low}$ cells from the chorion. Once the LD lin^- single-cell suspensions were obtained from the chorion, the cells were stained with anti-CD34-APC and anti-CD45-PE mAbs and sorted in a FACSAria cell sorter (BD Biosciences) as previously described (Barcena et al., 2009).

In vitro expansion of $CD34^{++}CD45^{low}$ cells for fluorescent in situ hybridization (FISH). 1 x 10^4 sorted $CD34^{++}CD45^{low}$ cells from a 18.3 wks chorion (CP + SC) specimen were cultured in 48-well plates (BD Falcon, BD Biosciences), in 0.5 ml of Stem Span II medium (StemCell Technologies, Inc.) supplemented with 50 ng/ml of Kit ligand (KL) + 100 ng/ml of FLT-3 ligand (FL) + 20 ng/ml Thrombopoietin (TPO) + 20 ng/ml of interleukin-3 (IL-3). All the cytokines were from Peprotech Inc. (Rocky Hill, NJ), except FL, which was purchased from ORF Genetics (Kopavogur, Iceland). After 3.5 days in culture at 37°C, 5%CO_2, the cells were harvested, fixed and deposited on slides for FISH.

FISH. 2-10 x 10^3 sorted cells were processed immediately after their isolation and FISH was performed using the X chromosome-specific probe [Vysis CEP X (DXZ1) SpectrumGreen] and the Y chromosome-specific probe [CEP Y (DYZ3) SpectrumOrange] from Abbott Molecular (Abbott Park, IL) following manufacturer's protocol and as previously reported (Qi et al., 2015). For additional details, please see Supplemental methods. The cells were stained with DAPI II (Abbott Molecular) to visualize nuclei. FISH results were analyzed and documented by using the CytoVision system (Leica Microsystems, Buffalo Grove, IL).

Acknowledgements

We thank the staff and faculty at San Francisco General Hospital Women's Options Center for assistance in the collection of early gestation extraembryonic tissues. We thank Ms. Jean Perry (RN MS NP, UCSF, Department of Obstetrics, Gynecology and Reproductive Sciences) for assistance in obtaining the equivalent tissues at term. We are grateful to Mr. Gabriel A. Goldfien and Mr. Jason Farrell for assisting in sample collection. We also wish to thank Ms. Katharine Sutliff, (Senior Scientific Illustrator, SCIENCE/AAAS) for the drawing of a human fetus in Fig. 1A.

Competing interest

No competing interests declared by all the authors.

Author Contributions

AB, conception, design, execution and interpretation of the data. MOM and MK equally contributed to the design and execution of the experiments. AGG, MEF, AIB and KLP, ZQ and MG, execution of the experiments. HS, acquisition of samples. AB, MOM and SJF, drafting or revising the article.

Financial Support

This work was supported by grants from the National Blood Foundation (A.B.), and the National Institutes of Health: NIH/R21HD055328 (A.B.), NIH/1P01 DK088760-02 (M.O.M), NIH/1R56 AI101130-01 (S.J.F.) and Blood Systems Inc. The content is solely the responsibility of the authors and does not necessarily represent the official views of the National Institute of Diabetes and Digestive and Kidney Diseases or the National Institutes of Health. A.G.G. and A.I.B. were supported by a Bridges to Stem Cell Training grant TB1-01188 from the California Institute of Regenerative Medicine.

References

Aiuti, A., Webb, I. J., Bleul, C., Springer, T. and Gutierrez-Ramos, J. C. (1997). The chemokine SDF-1 is a chemoattractant for human CD34+ hematopoietic progenitor cells and provides a new mechanism to explain the mobilization of CD34+ progenitors to peripheral blood. *J Exp Med* **185**, 111-120.

Albelda, S. M., Oliver, P. D., Romer, L. H. and Buck, C. A. (1990). EndoCAM: a novel endothelial cell-cell adhesion molecule. *J Cell Biol* **110**, 1227-1237.

Barcena, A., Muench, M. O., Kapidzic, M. and Fisher, S. J. (2009). A new role for the human placenta as a hematopoietic site throughout gestation. *Reprod Sci* **16**, 178-187.

Barcena, A., Muench, M. O., Kapidzic, M., Gormley, M., Goldfien, G. A. and Fisher, S. J. (2011). Human placenta and chorion: potential additional sources of hematopoietic stem cells for transplantation. *Transfusion* **51 Suppl 4**, 94S-105S.

Bárcena, A., Park, S. W., Banapour, B., Muench, M. O. and Mechetner, E. B. (1996). Expression of Fas/CD95 and bcl-2 in primitive hematopoietic progenitors in the human fetal liver. *Blood* **88**, 2013-2025.

Basu, S. and Broxmeyer, H. E. (2009). CCR5 ligands modulate CXCL12-induced chemotaxis, adhesion, and Akt phosphorylation of human cord blood CD34+ cells. *J Immunol* **183**, 7478-7488.

Benirschke, K., Kaufmann, P. and Baergen, R. N. (2006). Anatomy and pathology of the placental membranes. In *Pathology of the human placenta*. New York: Springer

Bourne, G. (1962). The foetal membranes. A review of the anatomy of normal amnion and chorion and some aspects of their function. *Postgrad Med J* **38**, 193-201.

Broxmeyer, H. E., Orschell, C. M., Clapp, D. W., Hangoc, G., Cooper, S., Plett, P. A., Liles, W. C., Li, X., Graham-Evans, B., Campbell, T. B., et al. (2005). Rapid mobilization of murine and human hematopoietic stem and progenitor cells with AMD3100, a CXCR4 antagonist. *J Exp Med* **201**, 1307-1318.

Corbel, C., Salaun, J., Belo-Diabangouaya, P. and Dieterlen-Lievre, F. (2007). Hematopoietic potential of the pre-fusion allantois. *Dev Biol* **301**, 478-488.

Cross, J. C. (1998). Formation of the placenta and extraembryonic membranes. *Ann N Y Acad Sci* **857**, 23-32.

de Wynter, E. A., Durig, J., Cross, M. A., Heyworth, C. M. and Testa, N. G. (1998). Differential response of CD34+ cells isolated from cord blood and bone marrow to MIP-1 alpha and the expression of MIP-1 alpha receptors on these immature cells. *Stem Cells* **16**, 349-356.

de Wynter, E. A., Heyworth, C. M., Mukaida, N., Matsushima, K. and Testa, N. G. (2001). NOD/SCID repopulating cells but not LTC-IC are enriched in human CD34+ cells expressing the CCR1 chemokine receptor. *Leukemia* **15**, 1092-1101.

Gekas, C., Dieterlen-Lievre, F., Orkin, S. H. and Mikkola, H. K. (2005). The placenta is a niche for hematopoietic stem cells. *Dev Cell* **8**, 365-375.

Goyama, S., Wunderlich, M. and Mulloy, J. C. (2015). Xenograft models for normal and malignant stem cells. *Blood* **125**, 2630-2640.

Guezguez, B., Campbell, C. J., Boyd, A. L., Karanu, F., Casado, F. L., Di Cresce, C., Collins, T. J., Shapovalova, Z., Xenocostas, A. and Bhatia, M. (2013). Regional localization within the bone marrow influences the functional capacity of human HSCs. *Cell Stem Cell* **13**, 175-189.

Hamilton, W. J. and Boyd, J. D. (1960). Development of the human placenta in the first three months of gestation. *J Anat* **94**, 297-328.
Hamilton, W. J. and Boyd, J. D. (1970). *The Human Placenta*. Cambridge: Heffer and Sons.
Hu, Y. and Smyth, G. K. (2009). ELDA: extreme limiting dilution analysis for comparing depleted and enriched populations in stem cell and other assays. *J Immunol Methods* **347**, 70-78.
Ilancheran, S., Moodley, Y. and Manuelpillai, U. (2009). Human fetal membranes: a source of stem cells for tissue regeneration and repair? *Placenta* **30**, 2-10.
Imai, Y., Shimaoka, M. and Kurokawa, M. (2010). Essential roles of VLA-4 in the hematopoietic system. *IntJ Hematol* **91**, 569-575.
Imanirad, P. and Dzierzak, E. (2013). Hypoxia and HIFs in regulating the development of the hematopoietic system. *Blood Cells Mol Dis* **51**, 256-263.
Ivanovs, A., Rybtsov, S., Welch, L., Anderson, R. A., Turner, M. L. and Medvinsky, A. (2011). Highly potent human hematopoietic stem cells first emerge in the intraembryonic aorta-gonad-mesonephros region. *J Exp Med* **208**, 2417-2427.
Kerre, T. C., De Smet, G., De Smedt, M., Offner, F., De Bosscher, J., Plum, J. and Vandekerckhove, B. (2001). Both CD34+38+ and CD34+38- cells home specifically to the bone marrow of NOD/LtSZ scid/scid mice but show different kinetics in expansion. *J Immunol* **167**, 3692-3698.
Kubota, Y., Takubo, K. and Suda, T. (2008). Bone marrow long label-retaining cells reside in the sinusoidal hypoxic niche. *Biochem Biophys Res Commun* **366**, 335-339.
Lamkhioued, B., Abdelilah, S. G., Hamid, Q., Mansour, N., Delespesse, G. and Renzi, P. M. (2003). The CCR3 receptor is involved in eosinophil differentiation and is up-regulated by Th2 cytokines in CD34+ progenitor cells. *J Immunol* **170**, 537-547.
Levesque, J. P., Hendy, J., Takamatsu, Y., Simmons, P. J. and Bendall, L. J. (2003). Disruption of the CXCR4/CXCL12 chemotactic interaction during hematopoietic stem cell mobilization induced by GCSF or cyclophosphamide. *JCI* **111**, 187-196.
Luckett, W. P. (1975). The development of primordial and definitive amniotic cavities in early Rhesus monkey and human embryos. *Am J Anat* **144**, 149-167.
Mayani, H., Dragowska, W. and Lansdorp, P. M. (1993). Characterization of functionally distinct subpopulations of CD34+ cord blood cells in serum-free long-term cultures supplemented with hematopoietic cytokines. *Blood* **82**, 2664-2672.
McKenzie, J. L., Takenaka, K., Gan, O. I., Doedens, M. and Dick, J. E. (2007). Low rhodamine 123 retention identifies long-term human hematopoietic stem cells within the Lin-CD34+CD38- population. *Blood* **109**, 543-545.
Muench, M. O., Beyer, A. I., Fomin, M. E., Thakker, R., Mulvaney, U. S., Nakamura, M., Suemizu, H. and Barcena, A. (2014). The adult livers of immunodeficient mice support human hematopoiesis: evidence for a hepatic mast cell population that develops early in human ontogeny. *PloS one* **9**, e97312.
Muench, M. O., Roncarolo, M. G. and Namikawa, R. (1997). Phenotypic and functional evidence for the expression of CD4 by hematopoietic stem cells isolated from human fetal liver. *Blood* **89**, 1364-1375.
Notta, F., Doulatov, S., Laurenti, E., Poeppl, A., Jurisica, I. and Dick, J. E. (2011). Isolation of single human hematopoietic stem cells capable of long-term multilineage engraftment. *Science* **333**, 218-221.

Ottersbach, K. and Dzierzak, E. (2005). The murine placenta contains hematopoietic stem cells within the vascular labyrinth region. *Dev Cell* **8**, 377-387.
Peled, A., Kollet, O., Ponomaryov, T., Petit, I., Franitza, S., Grabovsky, V., Slav, M. M., Nagler, A., Lider, O., Alon, R., et al. (2000). The chemokine SDF-1 activates the integrins LFA-1, VLA-4, and VLA-5 on immature human CD34(+) cells: role in transendothelial/stromal migration and engraftment of NOD/SCID mice. *Blood* **95**, 3289-3296.
Prakobphol, A., Genbacev, O., Gormley, M., Kapidzic, M. and Fisher, S. J. (2006). A role for the L-selectin adhesion system in mediating cytotrophoblast emigration from the placenta. *Dev Biol* **298**, 107-117.
Qi, Z., Jeng, L. J., Slavotinek, A. and Yu, J. (2015). Haploinsufficiency and triploinsensitivity of the same 6p25.1p24.3 region in a family. *BMC Med Genomics* **8**, 38.
Rhodes, K. E., Gekas, C., Wang, Y., Lux, C. T., Francis, C. S., Chan, D. N., Conway, S., Orkin, S. H., Yoder, M. C. and Mikkola, H. K. (2008). The emergence of hematopoietic stem cells is initiated in the placental vasculature in the absence of circulation. *Cell Stem Cell* **2**, 252-263.
Robin, C., Bollerot, K., Mendes, S., Haak, E., Crisan, M., Cerisoli, F., Lauw, I., Kaimakis, P., Jorna, R., Vermeulen, M., et al. (2009). Human placenta is a potent hematopoietic niche containing hematopoietic stem and progenitor cells throughout development. *Cell Stem Cell* **5**, 385-395.
Rodesch, F., Simon, P., Donner, C. and Jauniaux, E. (1992). Oxygen measurements in endometrial and trophoblastic tissues during early pregnancy. *Obstet Gynecol* **80**, 283-285.
Rosu-Myles, M., Khandaker, M., Wu, D. M., Keeney, M., Foley, S. R., Howson-Jan, K., Yee, I. C., Fellows, F., Kelvin, D. and Bhatia, M. (2000). Characterization of chemokine receptors expressed in primitive blood cells during human hematopoietic ontogeny. *Stem Cells* **18**, 374-381.
Serikov, V., Hounshell, C., Larkin, S., Green, W., Ikeda, H., Walters, M. C. and Kuypers, F. A. (2009). Human term placenta as a source of hematopoietic cells. *Exp Biol Med (Maywood)* **234**, 813-823.
Su, S., Mukaida, N., Wang, J., Zhang, Y., Takami, A., Nakao, S. and Matsushima, K. (1997). Inhibition of immature erythroid progenitor cell proliferation by macrophage inflammatory protein-1alpha by interacting mainly with a C-C chemokine receptor, CCR1. *Blood* **90**, 605-611.
Tanaka, Y., Hayashi, M., Kubota, Y., Nagai, H., Sheng, G., Nishikawa, S. and Samokhvalov, I. M. (2012). Early ontogenic origin of the hematopoietic stem cell lineage. *Proc. Natl. Acad. Sci.U.S.A.* **109**, 4515-4520.
Tarnowski, M., Liu, R., Wysoczynski, M., Ratajczak, J., Kucia, M. and Ratajczak, M. Z. (2010). CXCR7: a new SDF-1-binding receptor in contrast to normal CD34(+) progenitors is functional and is expressed at higher level in human malignant hematopoietic cells. *Eur J Haematol* **85**, 472-483.
Torossian, F., Anginot, A., Chabanon, A., Clay, D., Guerton, B., Desterke, C., Boutin, L., Marullo, S., Scott, M. G., Lataillade, J. J., et al. (2014). CXCR7 participates in CXCL12-induced CD34+ cell cycling through beta-arrestin-dependent Akt activation. *Blood* **123**, 191-202.

van der Loo, J. C., Xiao, X., McMillin, D., Hashino, K., Kato, I. and Williams, D. A. (1998). VLA-5 is expressed by mouse and human long-term repopulating hematopoietic cells and mediates adhesion to extracellular matrix protein fibronectin. *JCI* **102**, 1051-1061.
Varga, N. L., Barcena, A., Fomin, M. E. and Muench, M. O. (2010). Detection of human hematopoietic stem cell engraftment in the livers of adult immunodeficient mice by an optimized flow cytometric method. *Stem Cell Stud* **1**.
Zeigler, B. M., Sugiyama, D., Chen, M., Guo, Y., Downs, K. M. and Speck, N. A. (2006). The allantois and chorion, when isolated before circulation or chorio-allantoic fusion, have hematopoietic potential. *Development* **133**, 4183-4192.

Figures

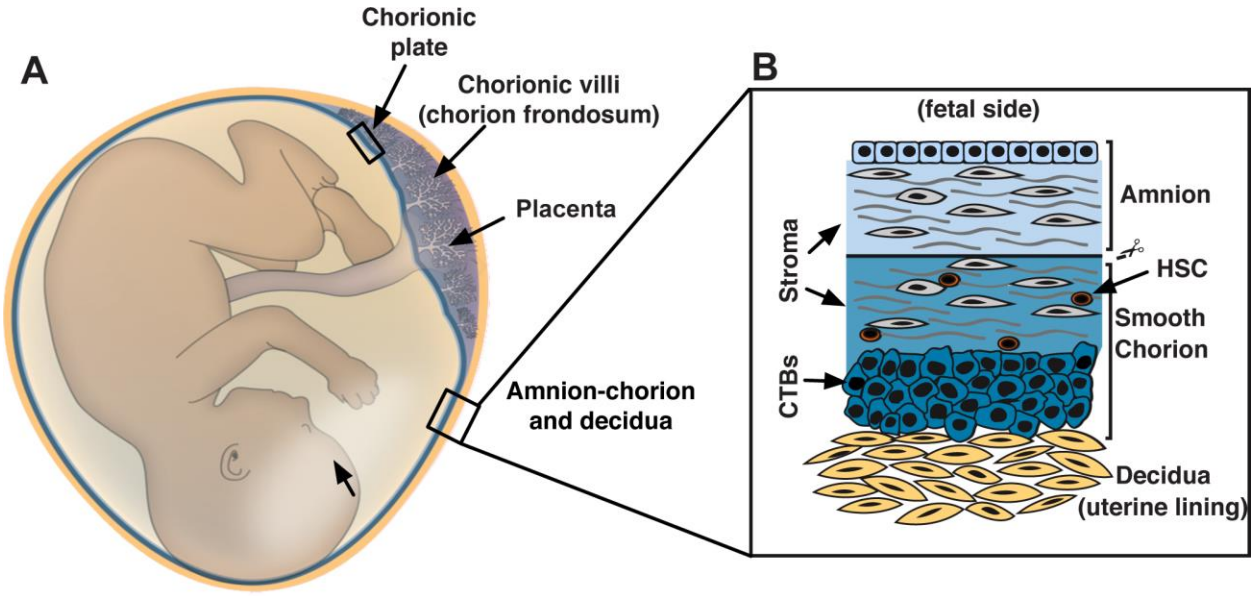

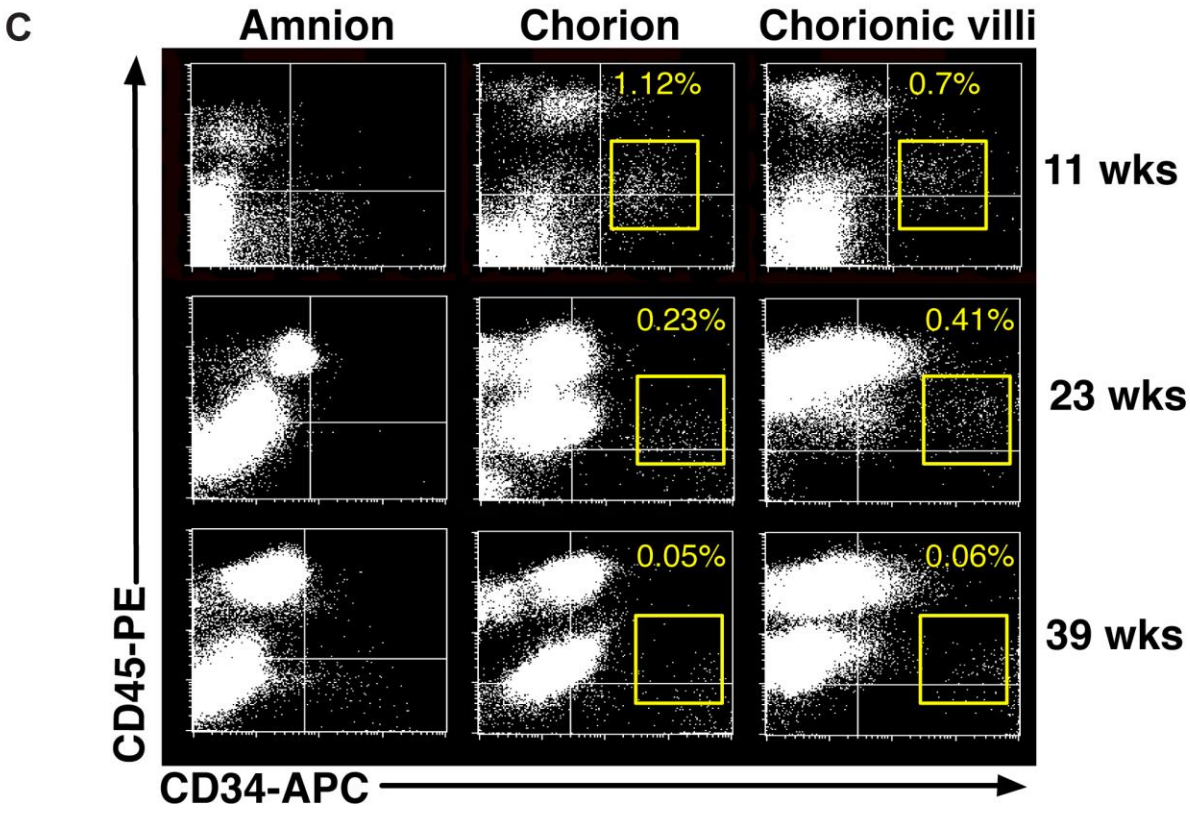

Figure 1. The human chorion contains HSCs. (A) Anatomy of the embryonic and extraembryonic compartments at mid-gestation. The placenta contains chorionic villi that protrude from the chorionic plate. The amnion-chorion is a bilayer (blue). The placenta and chorion are in direct contact with the decidua (yellow) (B) Basic histology of the amnion-smooth chorion (SC) at mid-gestation. The amnion (light blue) is composed of amniocytes, which line the amniotic cavity and an underlying stroma (grey cells). The SC, which shares the stroma (gray cells), contains multiple layers of cytotrophoblasts (CTBs, dark blue). The SC interfaces with the decidua (yellow). HSCs (brown cells) reside within the SC stroma. (C) Cell suspensions of freshly isolated amnion, chorion and chorionic villi were analyzed by FACS for CD34 and CD45 expression. Two x 10^5 viable cells were acquired and quadrants were set using isotype-matched controls. Yellow gates encompass the $CD34^{++}CD45^{low}$ cells. *n*=6 (1 x 1st trimester, 3 x 2nd trimester and 2 term). PE, phycoerythrin; APC, allophycocyanin.

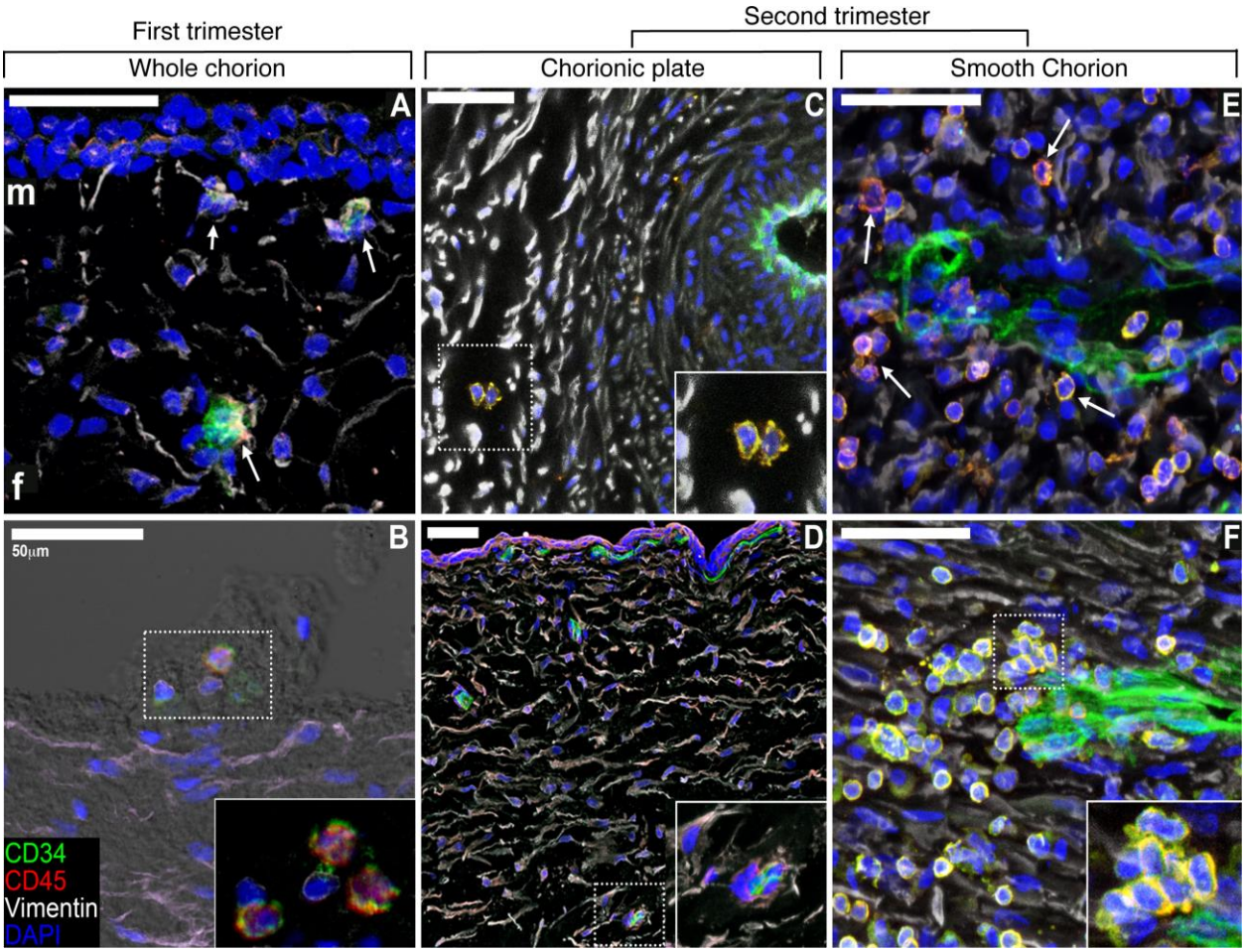

Figure 2. Immunolocalization analyses reveal the position of CD34^{++}CD45^{low} cells in 1st and 2nd trimester chorion. Tissue sections of chorion were stained for CD34 (green), CD45 (red) and vimentin (white) and visualized by confocal microscopy. The panels are oriented showing the fetal side (f) down and the maternal side up (m). Dotted white boxes indicate the position of the cells showed magnified in solid white boxes. Cells that co-expressed CD34 and CD45 were found, either individually or as clusters, amidst vimentin^{+} stromal cells (A-D). CD34^{+}CD45^{+} cells were also detected near blood vessels (E and F). (A) 5 wks whole chorion (*n*=3). (B) A small cluster of CD34^{+}CD45^{+} cells interact with vimentin^{+} stromal cells at the base of a villi in an 8 wks whole chorion (*n*=2). This section was visualized with differential interference contrast (DIC, gray scale). (C) CD34^{+}CD45^{+} cells in a 16 wks CP, *n*=4. (D) CD34^{+}CD45^{+} cells in a 23 wks CP (*n*=3). (E) CD34^{+}CD45^{+} cells SC from the same specimen shown in C, *n*=4. (F) CD34^{+}CD45^{+} cells in the CS from the same specimen shown in D, *n*=3.

Nuclei were visualized by staining with DAPI. Confocal images were obtained by sequential scanning of stained tissue sections. Scale bars in all the images represent 50 μm.

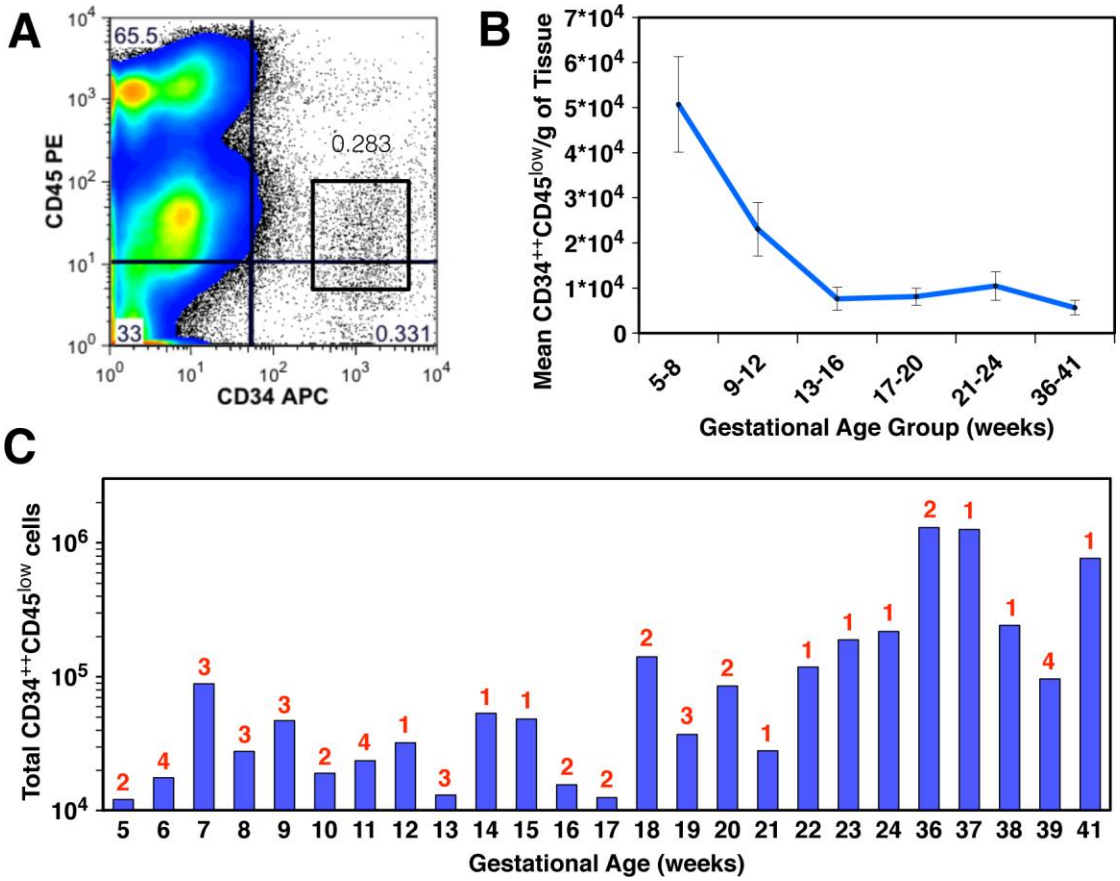

Figure 3. The density and total number of CD34^{++}CD45^{low} cells changes during development. Light density (LD) suspensions of chorionic cells (SC+CP) were isolated and stained with monoclonal antibodies (mAbs) against CD34, CD45, as well as isotype-matched control mAbs. (A) A representative analysis of a 18 wk chorion sample is shown, as well as the gate employed to determine the frequency of CD34^{++}CD45^{low} cells. (B) The density (mean number ± SEM/gram tissue) of CD34^{++}CD45^{low} cells at the indicated gestational windows is shown (*n*=51). (C) The total number of CD34^{++}CD45^{low} cells contained in chorion samples (*n*=51) at different gestational ages was calculated by multiplying the percentage of cells in the gate (shown in A) by the total number of cells (5-12 wks) or the number of light density cells (13-41 wks). The number of samples analyzed of each gestational age is indicated by red numbers atop each histogram bar.

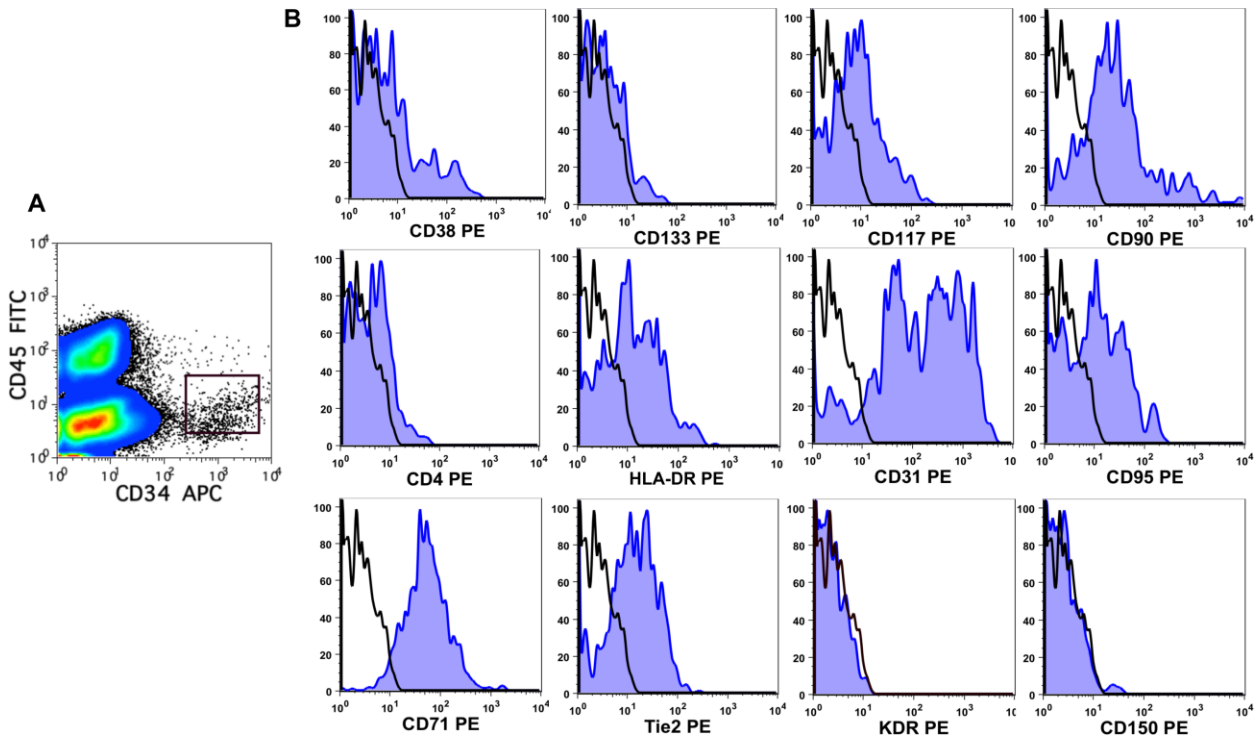

Figure 4. Phenotypic profile of chorionic CD34^{++}CD45^{low} cells. (A) LD suspensions of chorionic cells (19 wks of gestation) were stained with the indicated mAbs and PI. 1 x 10^6 viable cells were acquired for each analysis to ensure that at least 4 x10^3 events were included in the gate containing CD34^{++}CD45^{low} cells. (B) The expression of the indicated markers labeled with PE is shown as blue histograms outlined in dark blue. Data from the isotype-matched controls is overlaid as a clear histograms outlined in black. This experiment is representative of 3 experiments that analyzed the full marker set and 17 that analyzed a subset of the panel.

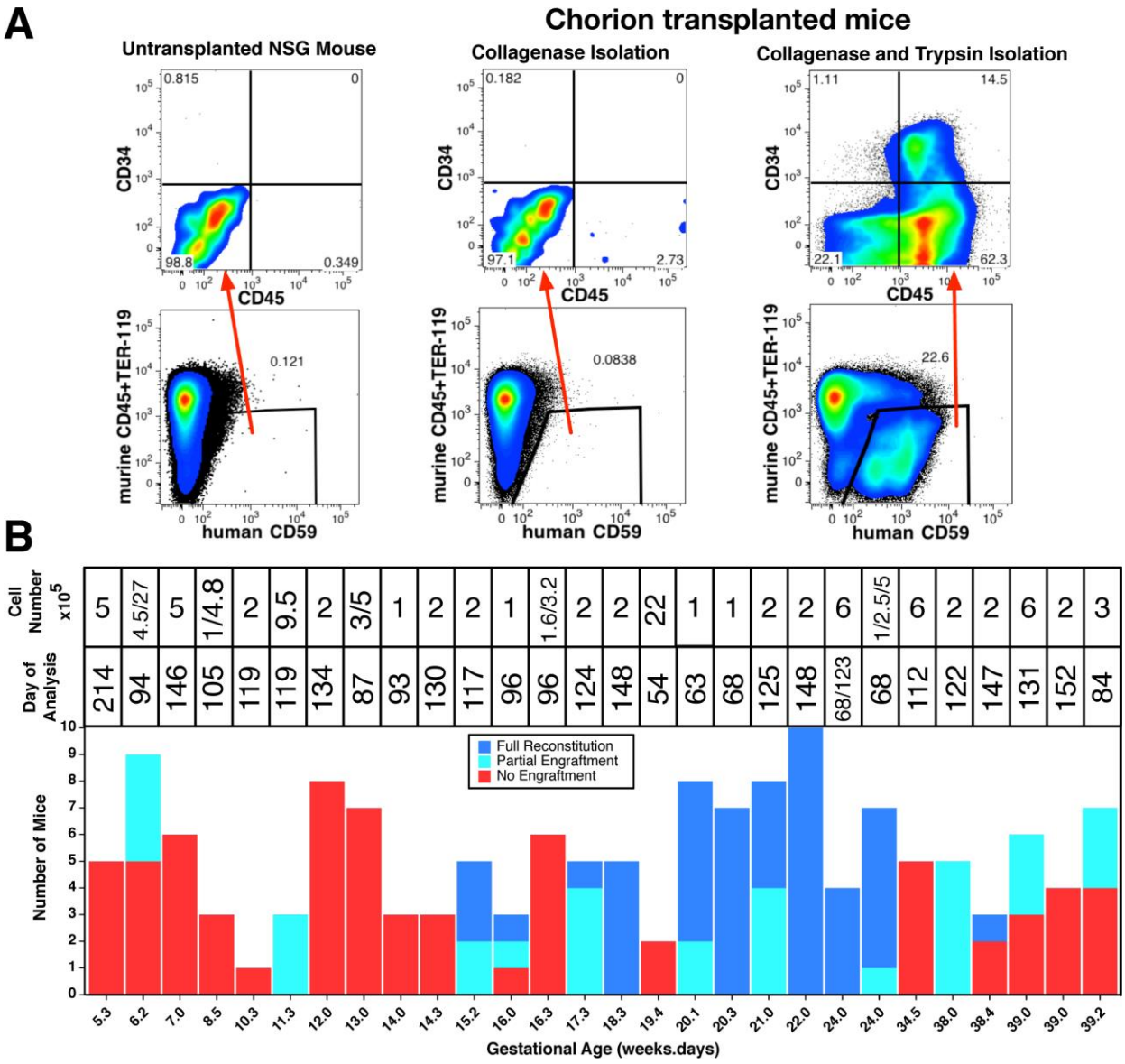

Figure 5. The engraftment potential of cells from the chorion peaks at mid-gestation and it is enabled by digestion with trypsin and collagenase. (A) 6 x 10^6 cells from a 24 wk specimen isolated using collagenase IA alone and 6 x 10^5 cells isolated by the two enzyme digestion method (trypsin and collagenase IA treatment) were transplanted into 4 mice and 2 mice, respectively. Engraftment was analyzed after 123 days with human cells defined by CD59 expression (see also Fig. S2A). (B) The number of full (dark blue) or partial (light blue) engrafted mice transplanted with chorion of different gestational ages (5.3- 39.2 wks) is shown. Red bars indicate no reconstitution. The number of mice transplanted is indicated on the y-axis and

gestational age is indicated in the x-axis (*n*=27). Each bar represents a single experiment. The number of cells transplanted and the day of analysis are atop each bar.

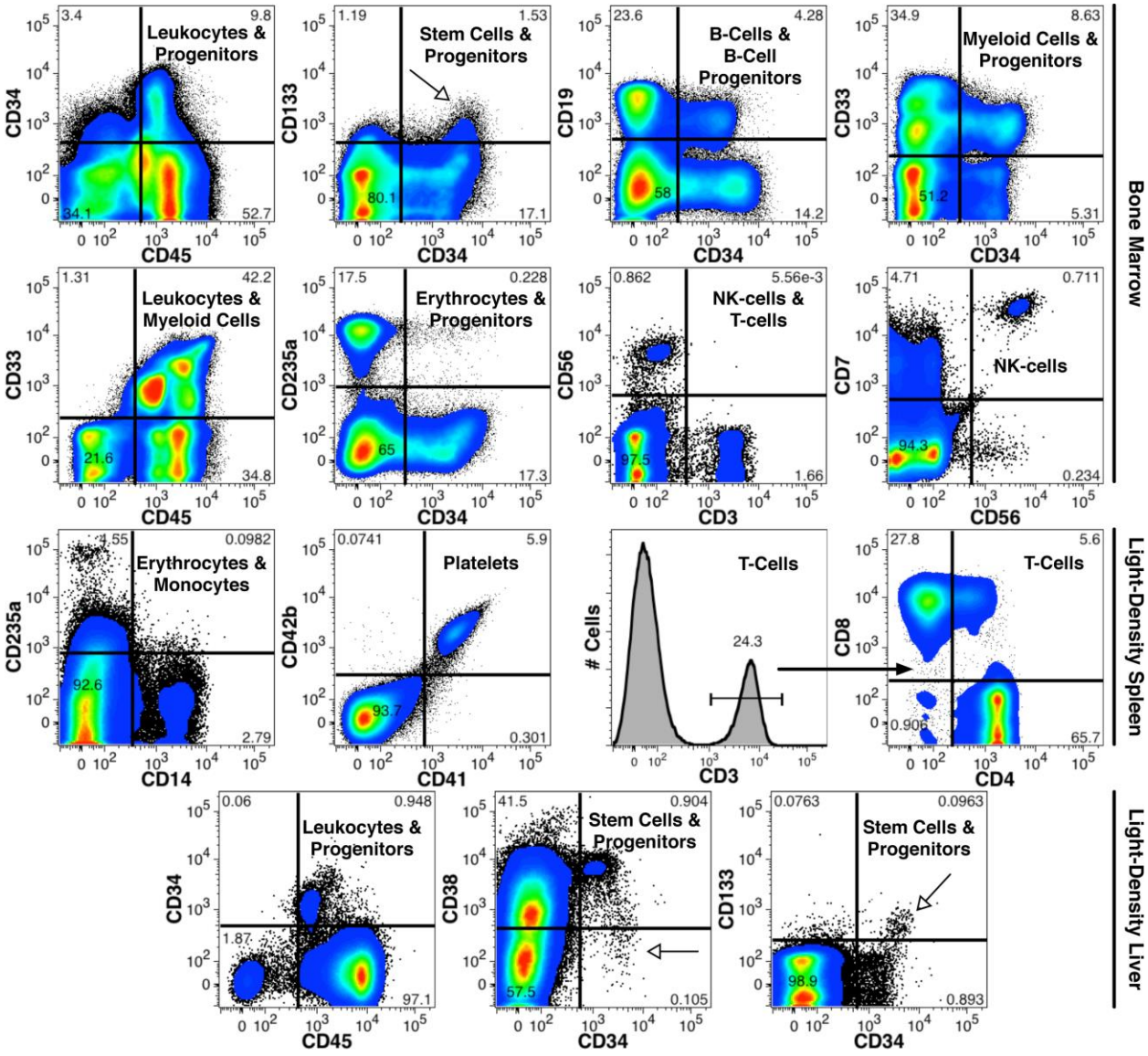

Figure 6. Multilineage engraftment by chorionic cells in mice. 2 x 10^5 LD, lin^- chorionic cells, 22 wks of gestation, were transplanted into NSG mice and analyzed 148 days later. BM, spleen and liver were analyzed by FACS using the indicated mAbs. Human chimerism in total BM was 58%, as measured by the percentage of human $CD59^+$ cells that lacked strong expression of mouse markers. Open arrows indicate the likely HSC population. The different hematopoietic lineages detected in the mouse organs among human $CD59^+$ cells are shown by the labeled FACS plots, indicating multilineage reconstitution (*n*=10).

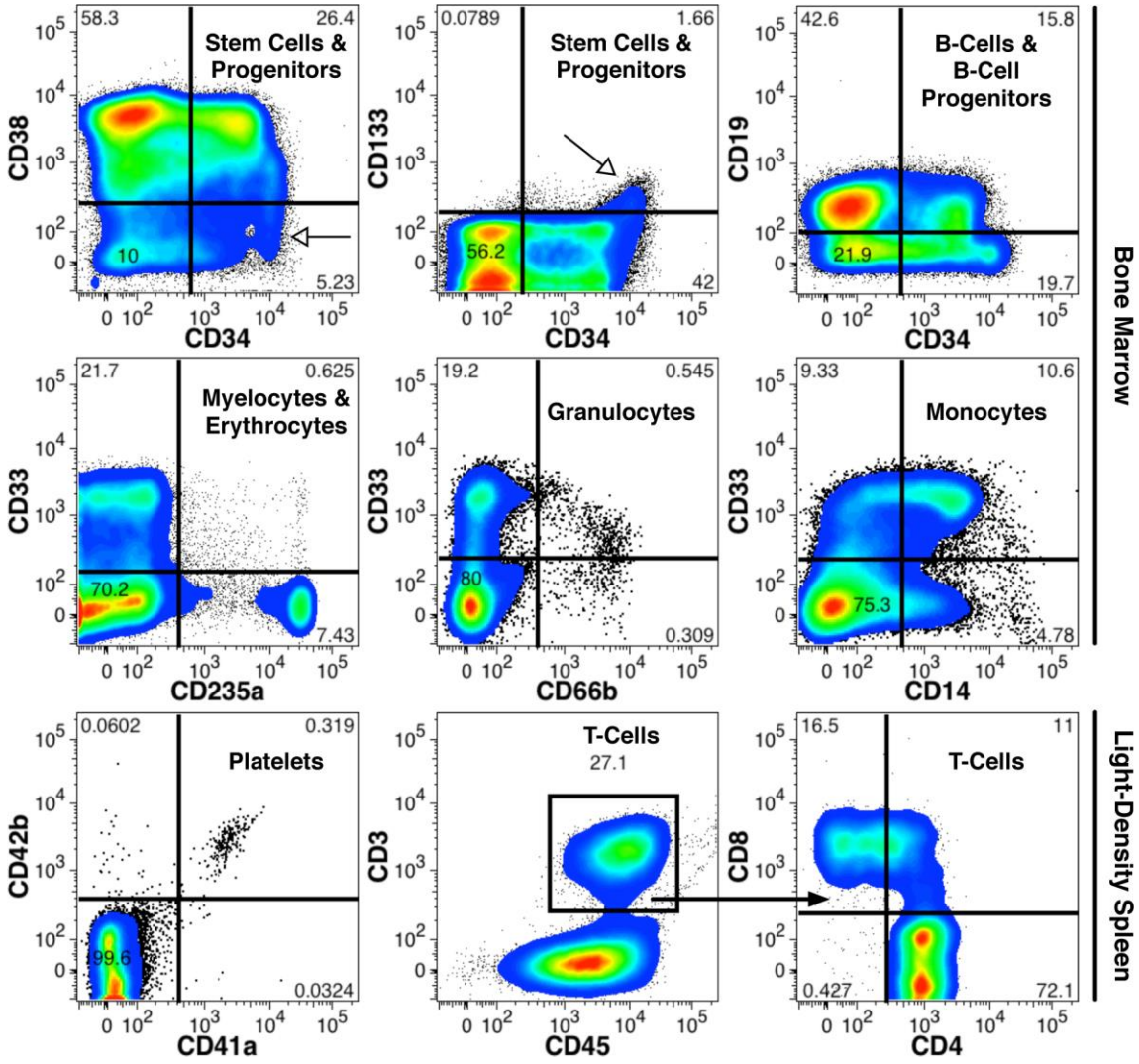

Figure 7. Chorionic cells engraft secondary recipients. LD, lin$^-$ chorionic cells, 24 wks of gestation, were transplanted into primary recipients. The BM was harvested 68 days later and re-transplanted. Total BM (top two rows) and LD spleen cells (bottom row) were analyzed 91 days after the second transplant. BM was engrafted with 21% human CD59$^+$ cells. The analytical strategy and data depiction were similar to Fig. 6. Open arrows indicate the likely presence of an HSC population. The FACS results indicated multilineage serial reconstitution from primary to secondary recipients (*n*=2).

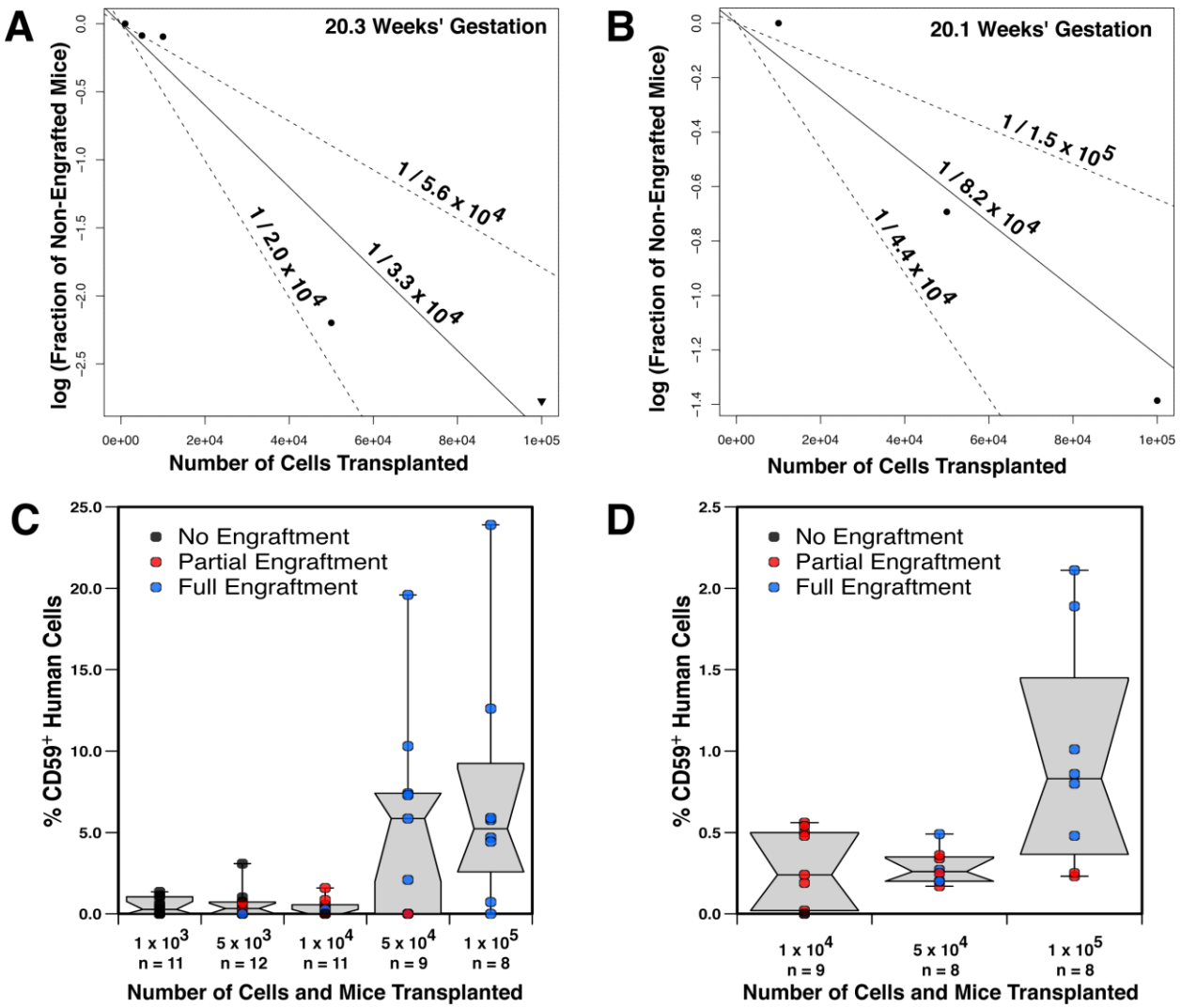

Figure 8. Enumeration of chorionic HSCs by ELDA. Mice were transplanted with varying doses of LD, lin$^-$ chorionic cells isolated from two mid-gestation tissues, indicated in the x-axis. Their BMs were analyzed for human cells at 63 (A) and 68 days (B) post-transplant. ELDA was performed and the estimated frequency and range (95% confidence interval) of HSCs is indicated. (C) Box plots of engraftment levels (%CD59$^+$ cells) for the experiment shown in A. (D) Box plots of engraftment levels (%CD59$^+$ cells) for the experiment shown in B. In C and D, the results obtained from individual mice are shown, indicating partial (red), full (blue) or no (black) multilineage engraftment.

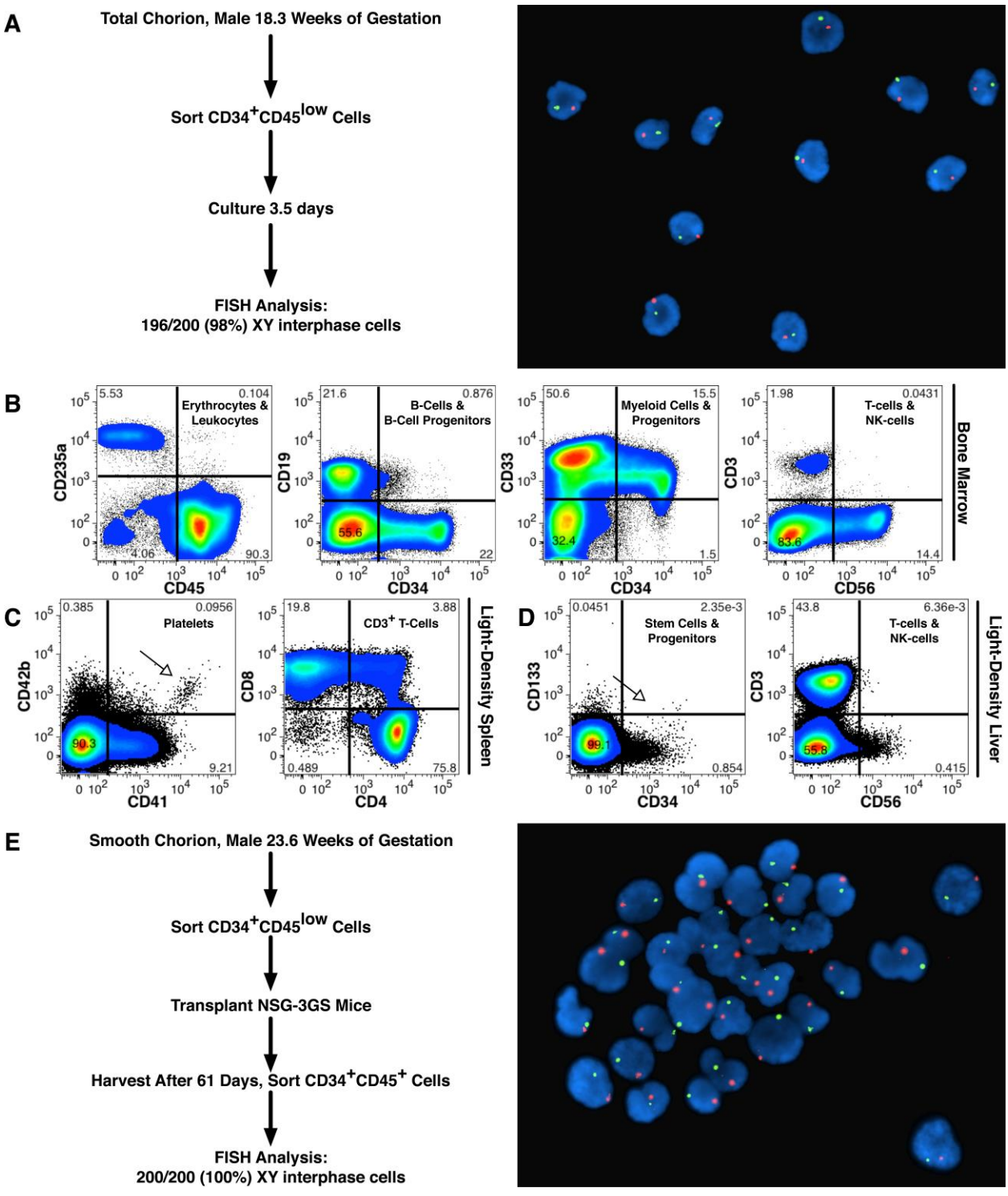

Figure 9. CD34^{++}CD45^{low} chorionic cells are of fetal origin and contain HSCs. (A) 1 x 10^4 CD34^{++}CD45^{low} cells were isolated by FACS from the CP + SC of a male fetus, 18.3 wks of gestation, and cultured for 3.5 days. FISH analysis showed that 98% of the interphase cells haf

a male (XY) signal. A photomicrograph of the cells that were analyzed is shown. $CD34^{++}CD45^{low}$ cells isolated from a male, 23.6 wks of gestation, SC were transplanted into NSG-3GS mice. Engraftment was analyzed 61 days later (n=4). Representative results showing hematopoietic engraftment of the BM (B), spleen (C) and liver (D) are shown. Open arrows indicate splenic platelets (C) and a likely population of HSC in the liver (D). The BM of 4 engrafted mice was pooled and $CD34^{++}CD45^{+}$ cells isolated by FACS, all of which were male based on FISH analysis. (E) A photomicrograph of $CD34^{++}CD45^{+}$ cells sorted from the mouse BM cells showed a male (XY) signal.

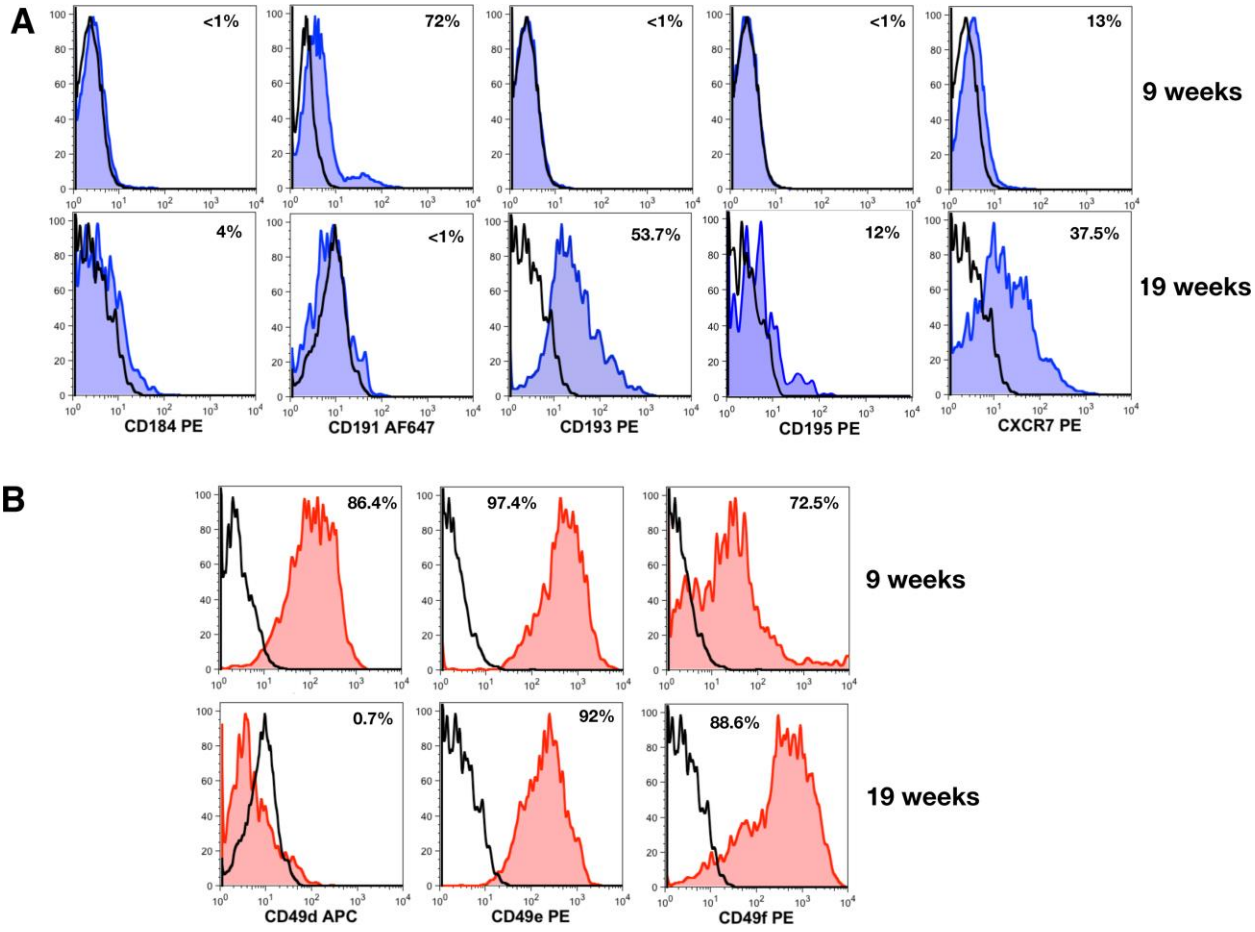

Figure 10. CD34^{++}CD45^{low} chorionic cells express several chemokine receptors and β1 integrins. (A) Freshly isolated LD suspensions of chorionic cells from 9 and 19 wk samples were stained with the indicated mAbs and PI. Similar to the analysis performed in Fig. 4, a gate was set to include CD34^{++}CD45^{low} cells. Their staining with mAbs against chemokine receptors (CD184 [CXCR4], CD193 [CCR3], CD195 [CCR5], CXCR7 and CD91 [CCR1]) and isotype-matched controls is shown. The expression of each marker in the PE and Alexa Fluor 647 (AF647) channels is shown as blue histograms outlined in blue overlaid with the data from the isotype-matched control mAbs (shown as white histograms outlined in black). This experiment is representative of the analysis of *n*=3 for 1st trimester and *n*=4 for 2nd trimester samples. (B) LD suspensions of chorionic cells from the same 9 and 19 wk specimens were stained with the indicated mAbs and PI. A gate was set to include CD34^{++}CD45^{low} chorionic cells (not shown) and their staining with mAbs against CD49d ($\alpha_4\beta_1$), CD49e ($\alpha_5\beta_1$) and CD49f ($\alpha_6\beta_1$) is shown in

red histograms overlaid with the data from the isotype-matched control mAbs (white histograms outlined in black; *n*=6, 3 from 1st trimester and 3 from 2nd trimester).

Supplemental Data

Supplemental Methods

Tissue processing. Samples of chorion comprised both the smooth chorion (SC) and the chorionic plate (CP), which was denuded of chorionic villi (Fig. S1A and B), unless otherwise specified that only the SC was used (Fig.9). Once that the tissues were dissected under a microscope, we processed them following a method previously described (Genbacev et al., 2011) that we modified to improve the recovery of hematopoietic cells (Barcena et al., 2009). Specifically, we added a final enzymatic digestion treatment of the chorion, amnion and chorionic villi preparations with 181 U/ml collagenase I-A, 0.12 mg/ml DNase I, 0.70 mg/ml hyaluronidase type I-S, and 1 mg/ml BSA in PBS at 37°C. Digestion continued for 5-60 min until total cellular dissociation was observed. For tissues 5-6 wks of gestational age, it was not possible to separate the membrane portion from the placental chorionic villi, therefore we prepared cells from whole chorion. In older specimens (≥ 7 wks) the CP was dissected from chorionic villi and those tissues were prepared separately. For 7-12 wks specimens, transplantation and FACS were performed on the dissociated cells without further fractionation. For samples older than 12 wks, the light-density (LD) fraction was obtained (by centrifugation over Nycoprep (1.077 g/ml; Greiner Bio-One, Monroe, NC) for 30 min (25°C) at 600 × *g*) for FACS and transplantation, as previously described (Barcena et al., 2009). For older samples (≥14 wks) in which the amnion has begun to fuse to the chorion, manual separation of these two membranes was performed, as shown macroscopically in Fig S1C and at a histological level in Fig. S1D and E (before and after amnion removal, respectively). This step was followed by enzymatic dissociation and isolation of the LD fraction was then subjected to our standard mature lineage(lin) depletion to enrich in hematopoietic progenitors prior to transplantation. The mAbs used for depletion were all unconjugated and obtained from BioLegend (San Diego, CA), used at 1μg/10^6 target cells, and recognized CD235a (erythrocytes), CD14 (macrophages), CD19 and CD29 (B cells), CD3 (T cells) and CD56 (NK cells). After washing to remove the excess unbound mAbs, the cells were subjected to negative magnetic selection by using BioMag magnetic beads coated with goat anti-mouse IgG antibody (Qiagen Inc., Germantown, MD). The resulting LD lin^- cell suspension was

counted and transplanted into mice. For FACS analyses, no lineage depletions were performed.

Human hematopoietic engraftment of mice. NSG-3GS mice were only used for the transplant experiment associated with the FISH analyses shown in Fig. 9; NSG mice were used in all other experiments. Mice were irradiated with 175 or 200 cGy using an RS2000 X-Ray Biological Irradiator (RAD Source Technologies, Inc., Alpharetta, GA, USA) 1 to 3 hours before the procedure. Female and male mice were transplanted as adults (≥8 wks old) by tail-vein injection using a 28g U100 insulin syringe (BD, Franklin Lakes, NJ, USA). The cells were suspended in 200 µL of PBS (Mediatech, Inc., Manassas, VA, USA). For several days before and for the first month after transplant, the standard chow was replaced with irradiated Global 2018 rodent diet with 4100 ppm Uniprim® (Harlan Laboratories, Inc., Hayward, CA, USA). Most of the transplanted mice were analyzed between 100 and 150 days post-transplant. Mice were sacrificed by carbon dioxide asphyxiation followed by cervical dislocation. BM was harvested by using a syringe with a 27-gauge needle to flush the femurs with approximately 3 ml of culture medium as described (Mahajan et al., 2015). Spleen and liver specimens were held in culture medium on ice until cell isolation. At the conclusion of each experiment, mice were examined for signs of poor health or pathologies such as tumors of the liver, spleen, and/or thymus. Any moribund animals were removed from the study. Mouse BM, spleen and liver were processed as previously described (Varga et al., 2010).

Immunolocalization and fluorescence microscopy. We applied previously reported methods (Prakobphol et al., 2006). The binding of antibodies that were not direct conjugates was detected by using the appropriate species-specific secondary antibody, a rhodamine-conjugated donkey anti-mouse IgG for anti-CD45 (Jackson ImmunoResearch Laboratories Inc., West Grove, PA) and AF 633-conjugated goat-anti-rabbit IgG for anti-vimentin (Invitrogen). As controls, serial sections were stained with the secondary antibody alone or mouse-IgG_1-FITC (BD Pharmingen).

FISH. In brief, 2-10 x 10^3 sorted cells were placed in ice cold fresh fixative (v/v 3:1 methanol:acetic acid) for 30 minutes at 4°C. Then the cells were dropped onto a slide and dried under controlled conditions (25°C, 38% relative humidity). We performed FISH using X-and Y-chromosome specific probes following manufacturer's protocol

(Abbott Molecular) and methods we have previously reported (Qi et al., 2015).

Supplemental References

Barcena, A., Muench, M. O., Kapidzic, M. and Fisher, S. J. (2009). A new role for the human placenta as a hematopoietic site throughout gestation. *Reprod Sci* **16**, 178-187.

Genbacev, O., Donne, M., Kapidzic, M., Gormley, M., Lamb, J., Gilmore, J., Larocque, N., Goldfien, G., Zdravkovic, T., McMaster, M. T., et al. (2011). Establishment of human trophoblast progenitor cell lines from the chorion. *Stem Cells* **29**, 1427-1436.

Mahajan, M. M., Cheng, B., Beyer, A. I., Mulvaney, U. S., Wilkinson, M. B., Fomin, M. E. and Muench, M. O. (2015). A quantitative assessment of the content of hematopoietic stem cells in mouse and human endosteal-bone marrow: a simple and rapid method for the isolation of mouse central bone marrow. *BMC Hematol* **15**, 9.

Prakobphol, A., Genbacev, O., Gormley, M., Kapidzic, M. and Fisher, S. J. (2006). A role for the L-selectin adhesion system in mediating cytotrophoblast emigration from the placenta. *Dev Biol* **298**, 107-117.

Qi, Z., Jeng, L. J., Slavotinek, A. and Yu, J. (2015). Haploinsufficiency and triploinsensitivity of the same 6p25.1p24.3 region in a family. *BMC Med Genomics* **8**, 38.

Varga, N. L., Barcena, A., Fomin, M. E. and Muench, M. O. (2010). Detection of human hematopoietic stem cell engraftment in the livers of adult immunodeficient mice by an optimized flow cytometric method. *Stem Cell Stud* **1**.

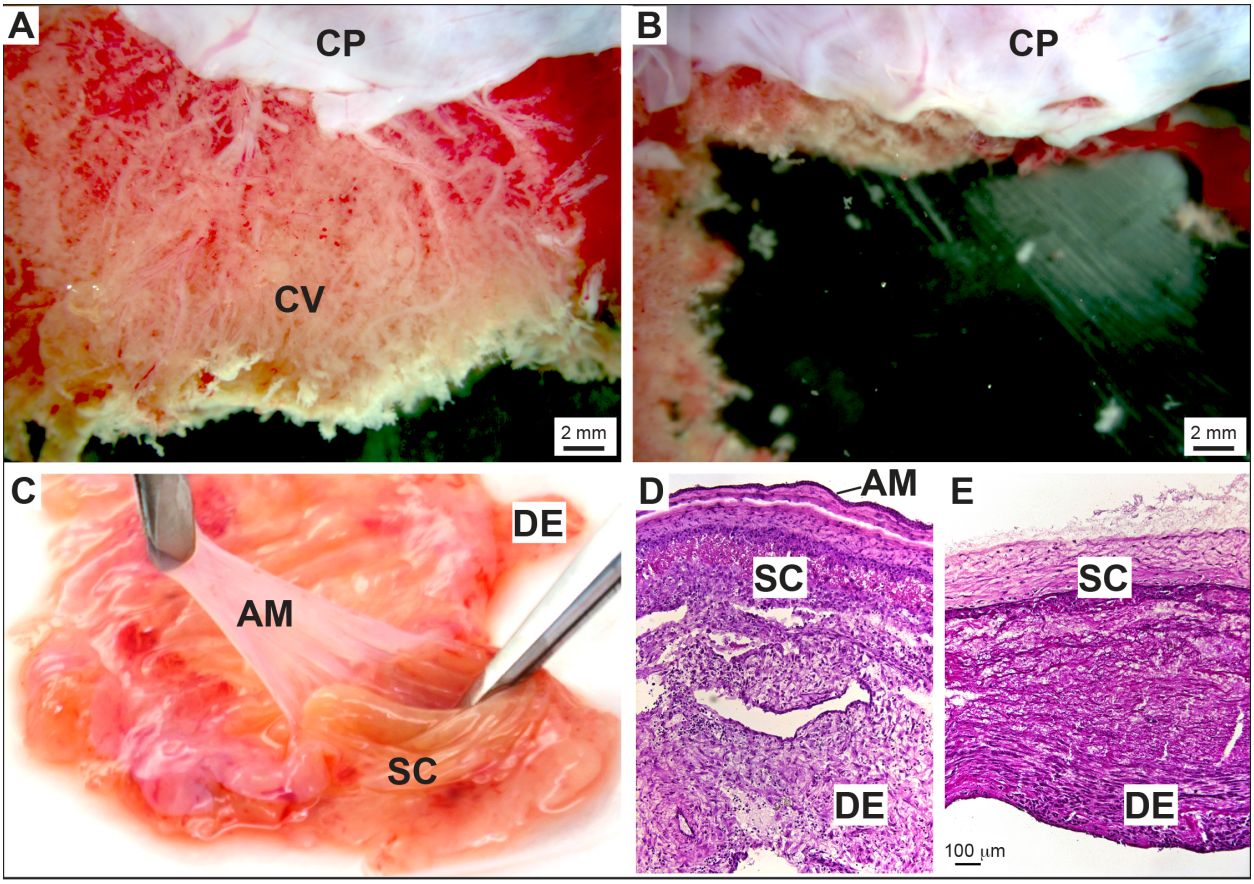

Supplemental Figure S1. Dissection and histology of the fetal human membranes. **A**. A portion of the chorionic plate (CP) of a 19 wk specimen is visualized under a dissection microscope and is shown intact (with the chorionic villi (CV) attached). After dissecting the CV, we obtain the denuded chorion, which is the CP without the CV (**B**). **C.** Manual separation of the amnion (AM) from the smooth chorion (SC) of a 22 wk specimen. A tissue section of the 22 wk amniochorion stained with hematoxylin and eosin is shown prior the removal of the amnion (**D**) and after the removal of the amnion (**E**). On the maternal side of the fetal membrane is the decidua (DE), which is manually removed prior the cell isolation.

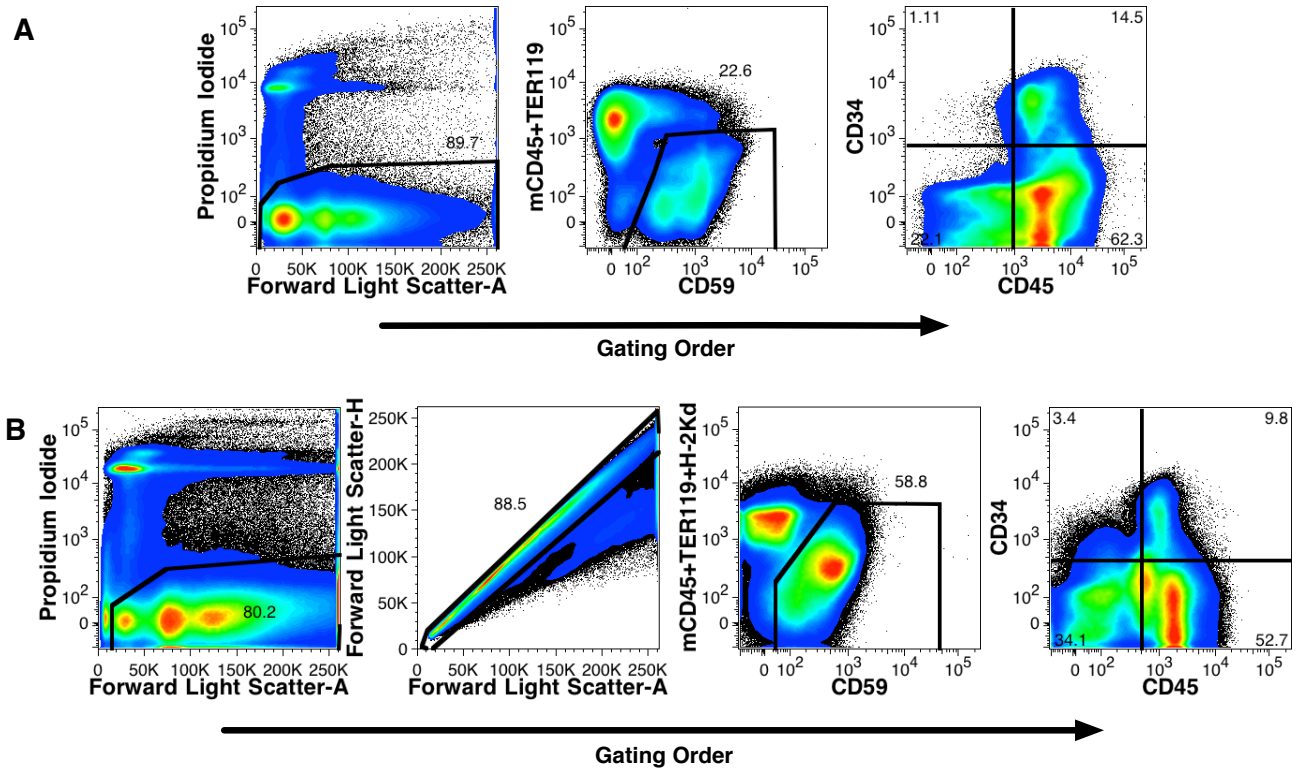

Supplemental Figure S2. Complete gating strategy used to define human cells in mouse BM. A. Live human cells were defined by their expression of CD59 and lack of expression of mouse markers, as well as the lack of propidium iodide staining as indicated in the gates. In some early studies the mouse markers were limited to CD45 and TER119, whereas the class I major histocompatibility antigen H-2k^{d} was stained in later experiments to further stain non-hematopoietic cells of mouse origin (**B**). Additionally, the use of forward-light scatter area (A) and height (H) parameters to exclude doublets was employed in some later analyses. Data shown correspond to engraftment data shown in Figs. 5A (**A**) and 6 (**B**).

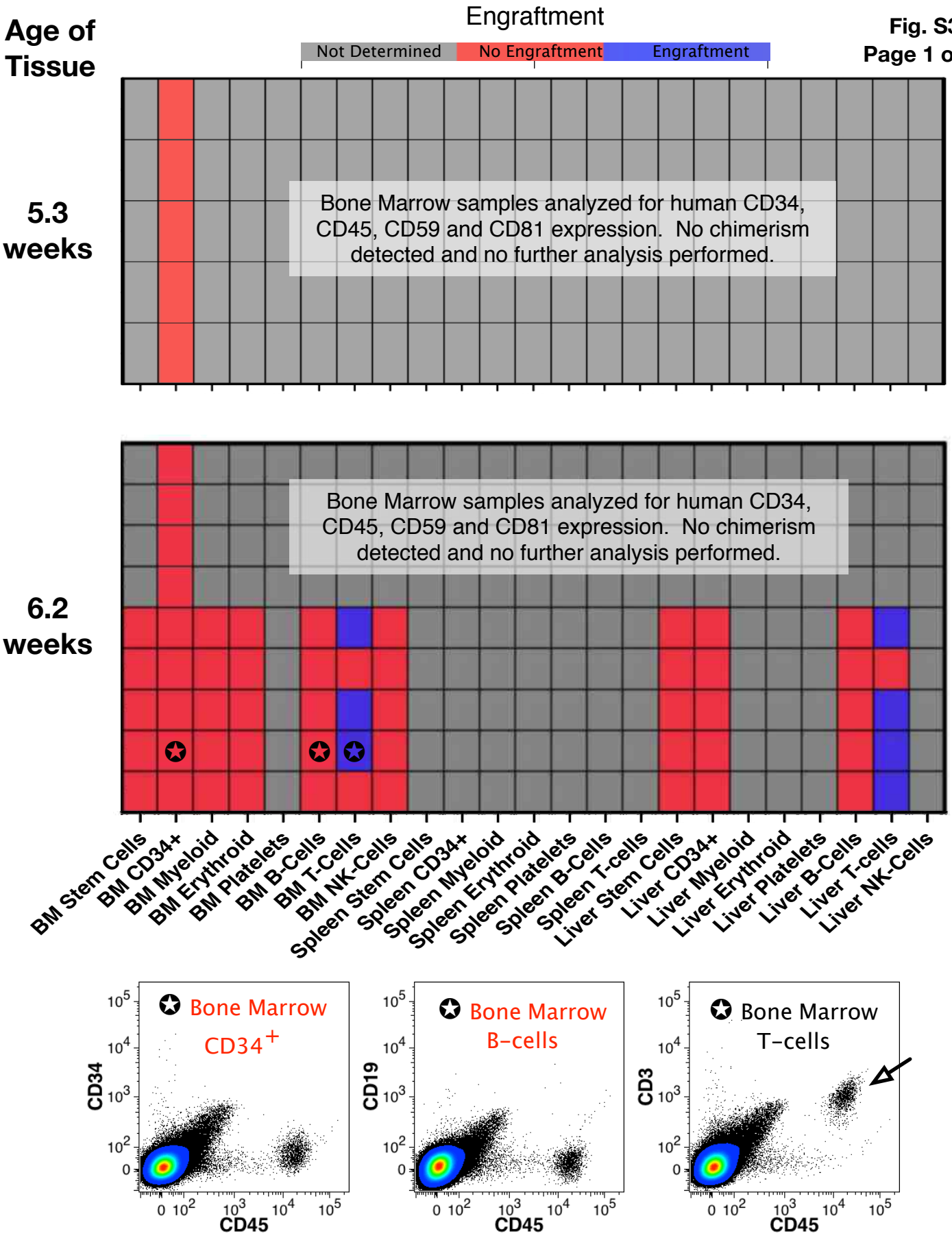

Results for Individual Mice

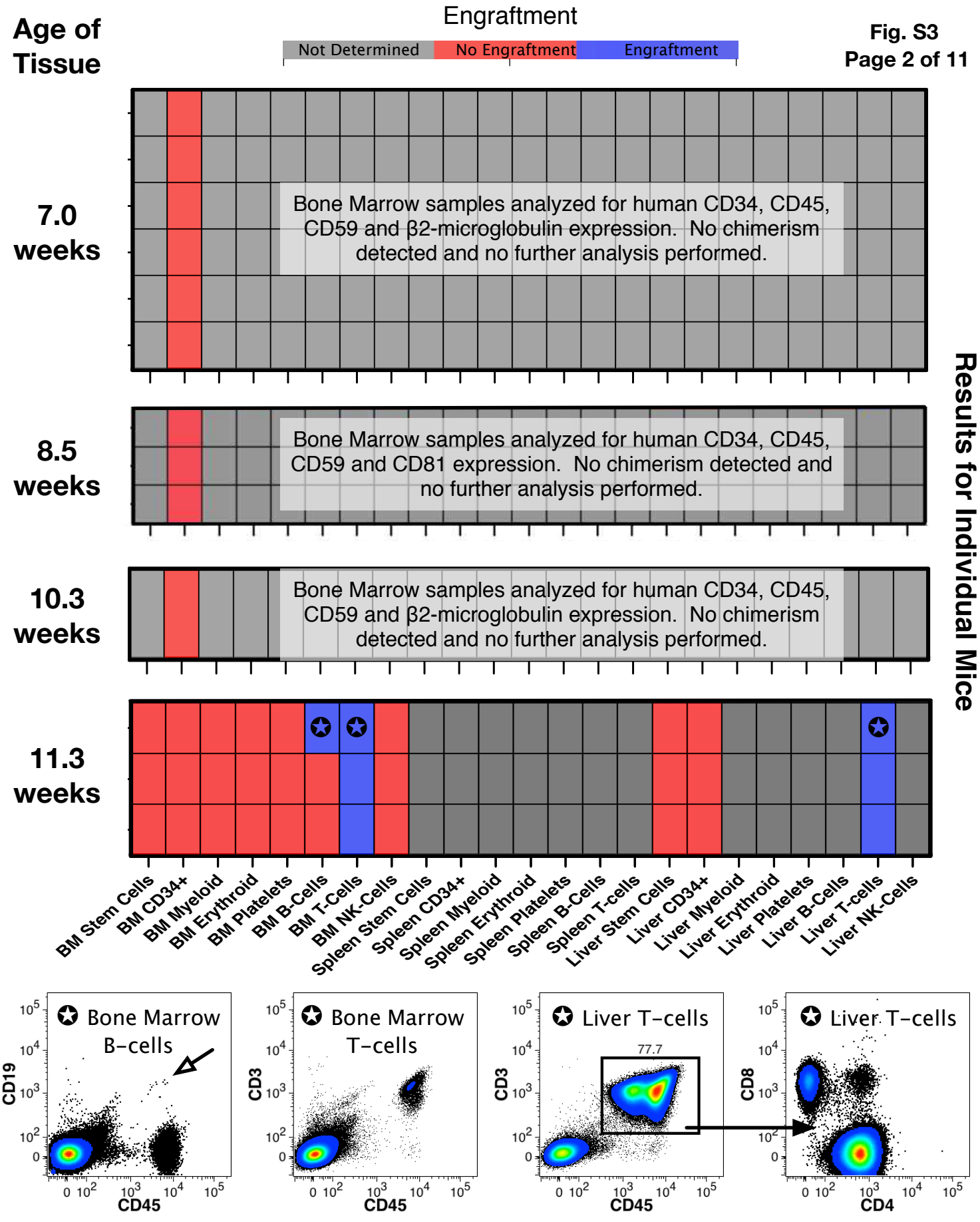

Tissue and Cell Population Analyzed

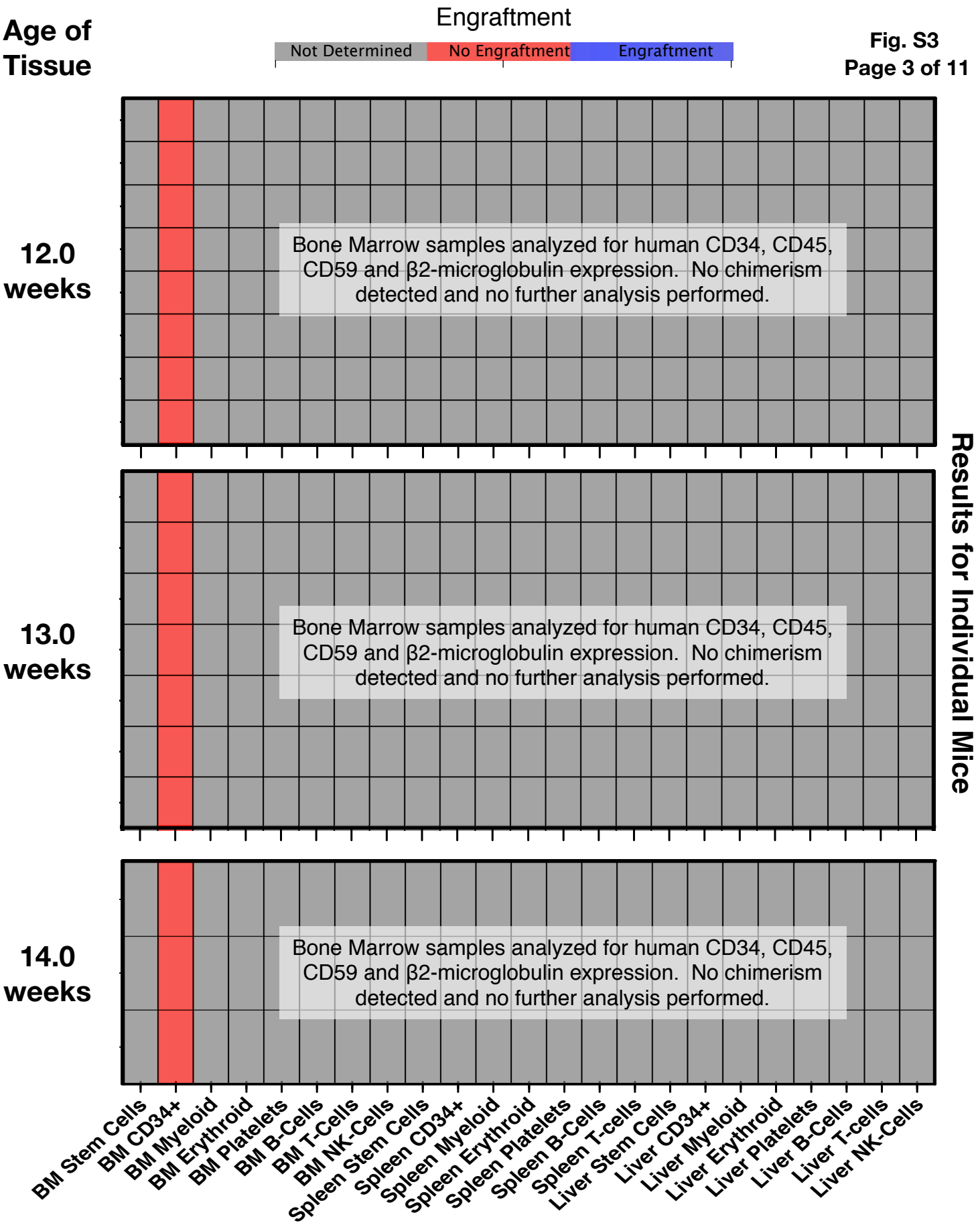

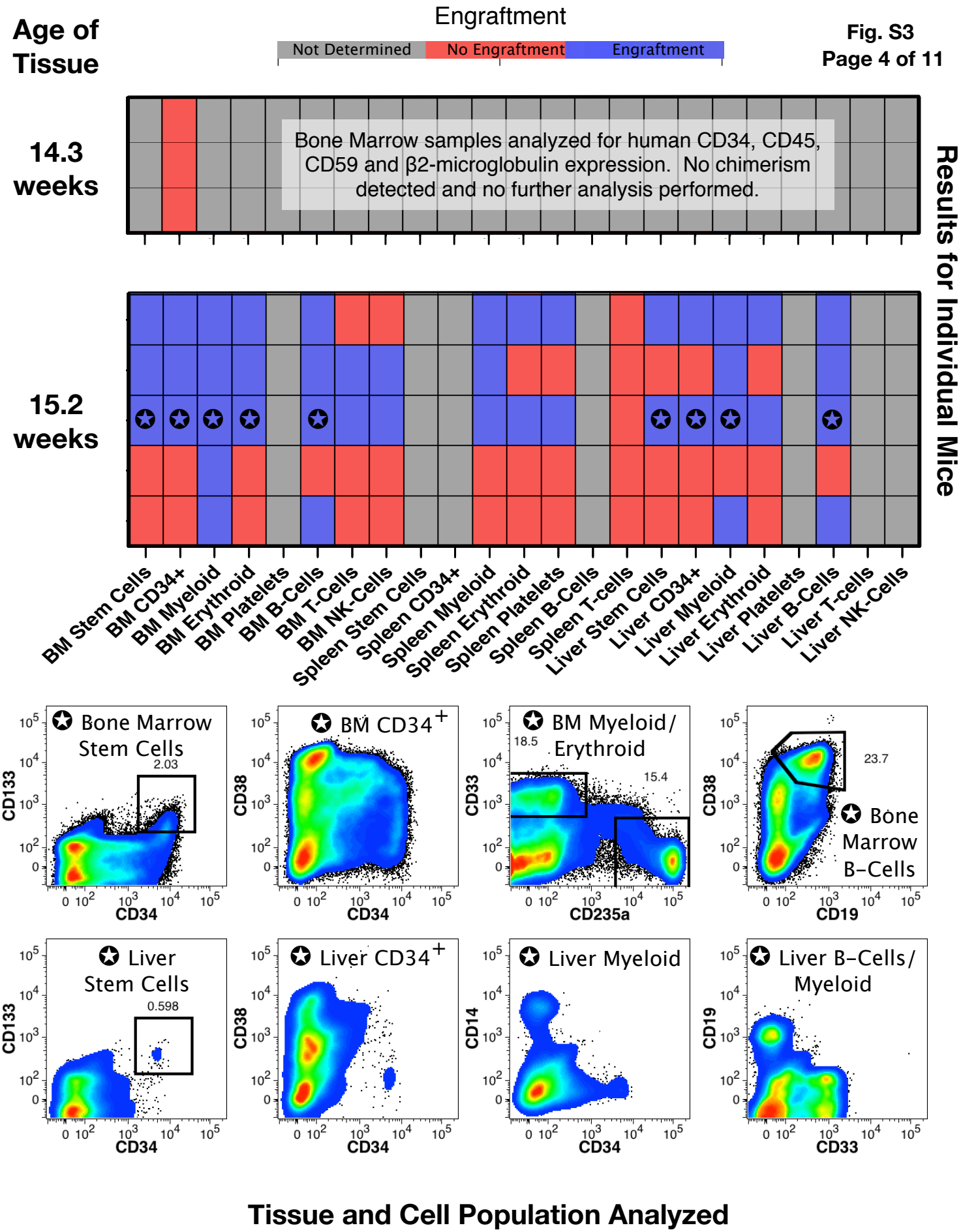

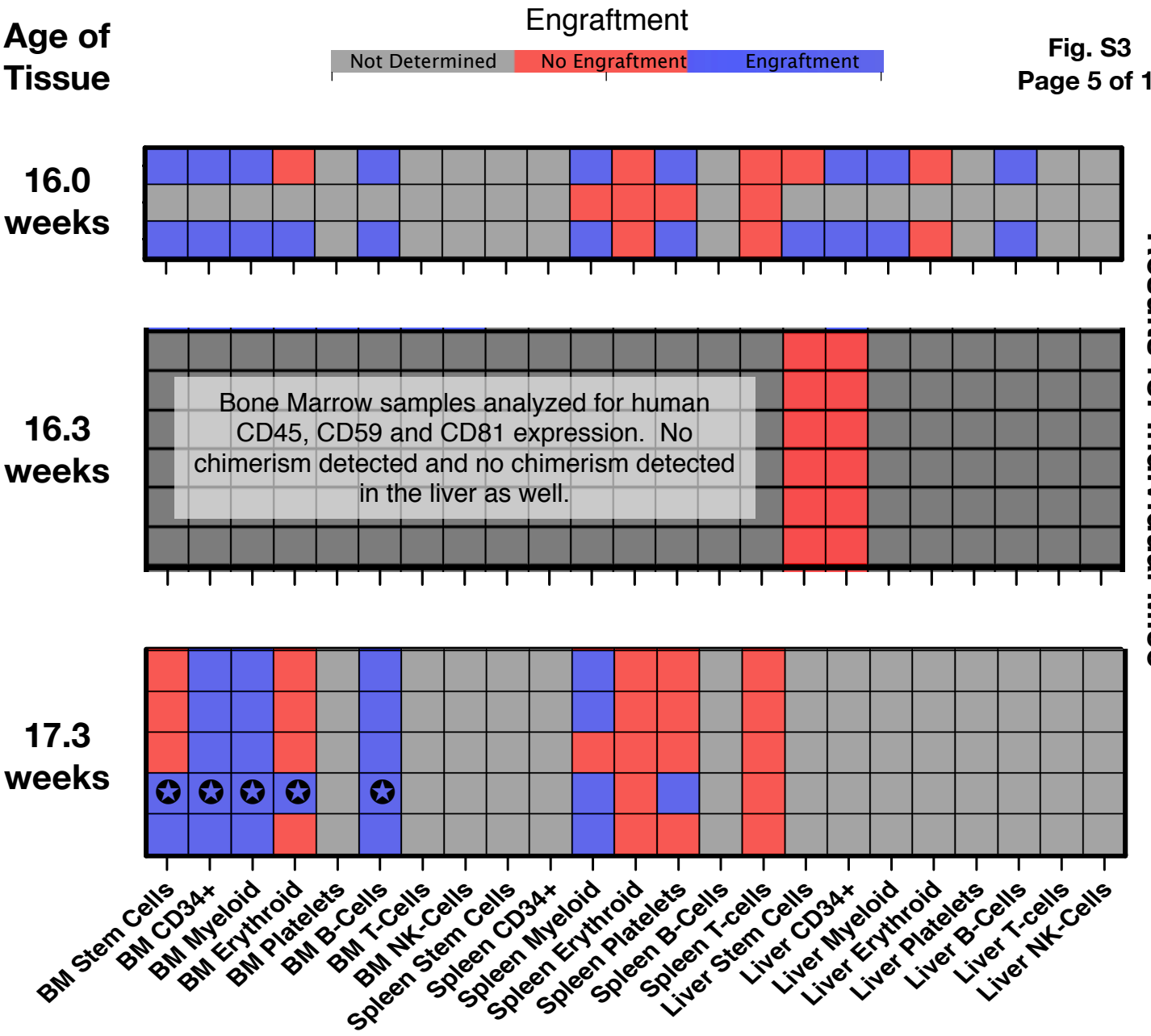

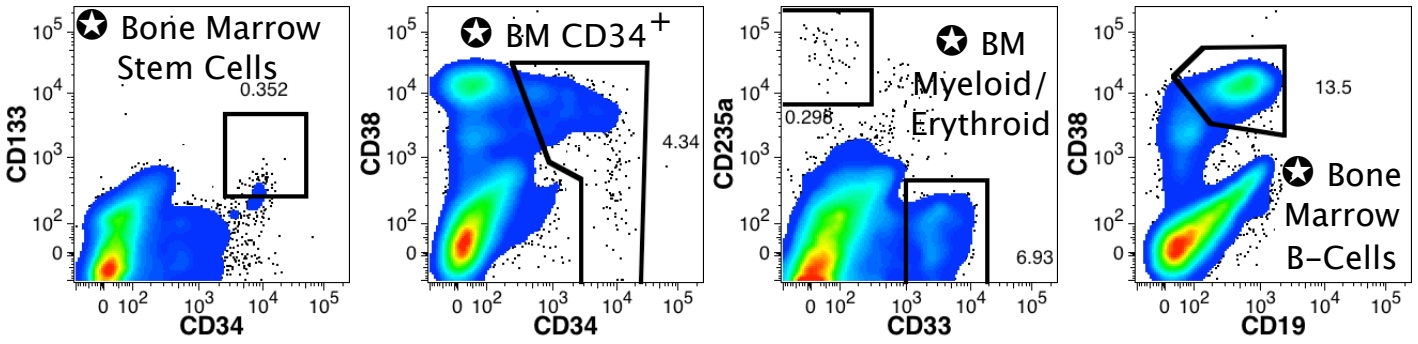

Tissue and Cell Population Analyzed

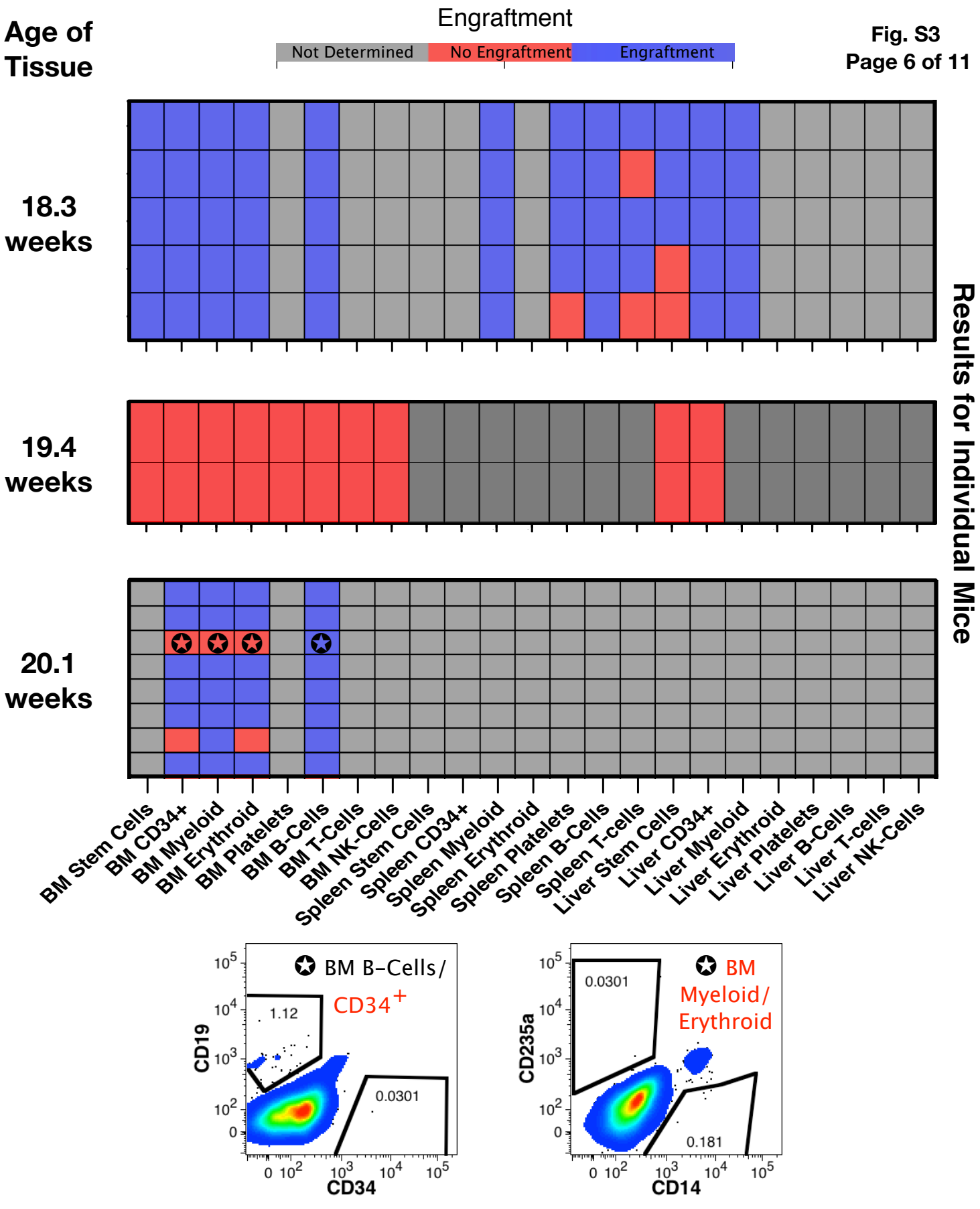

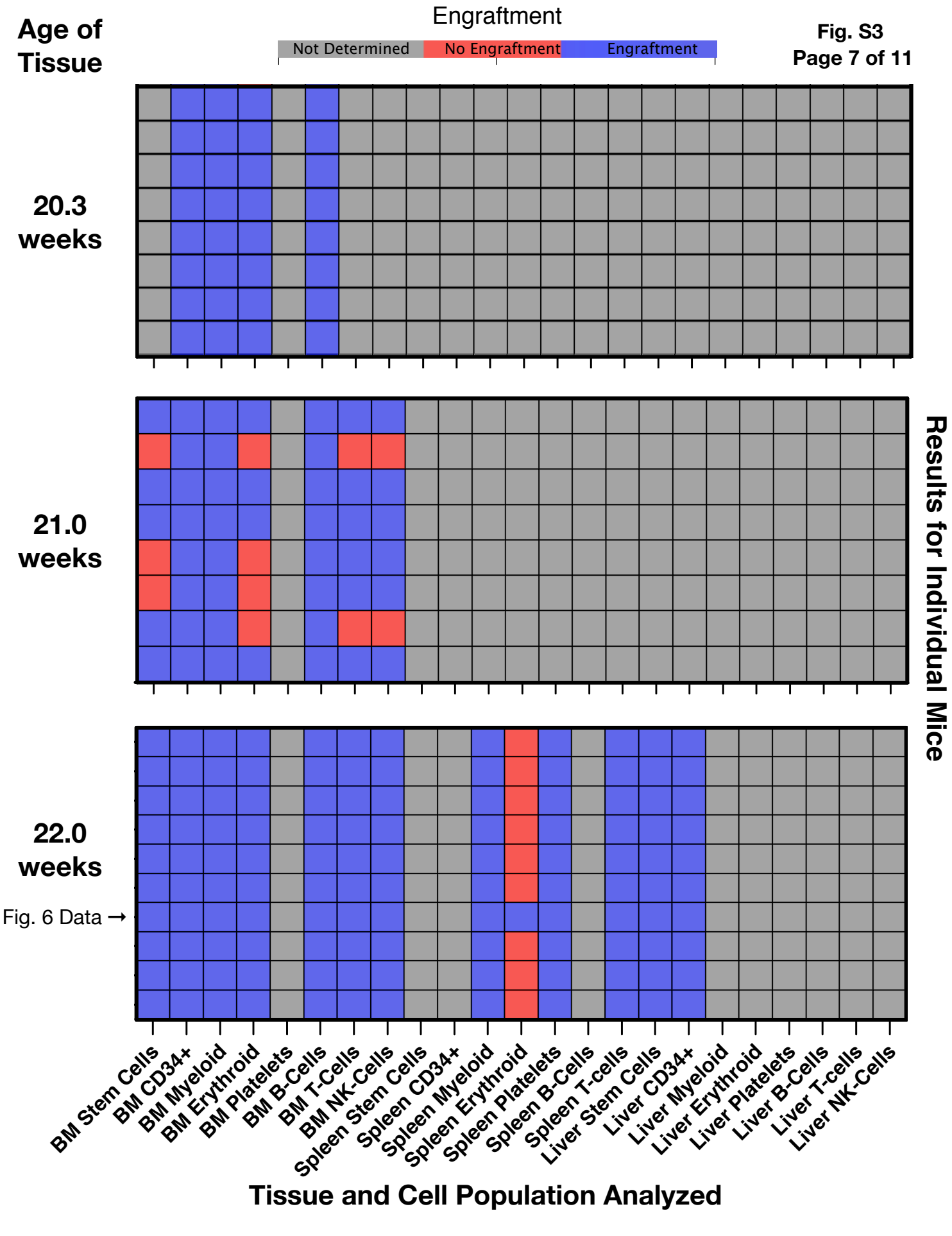

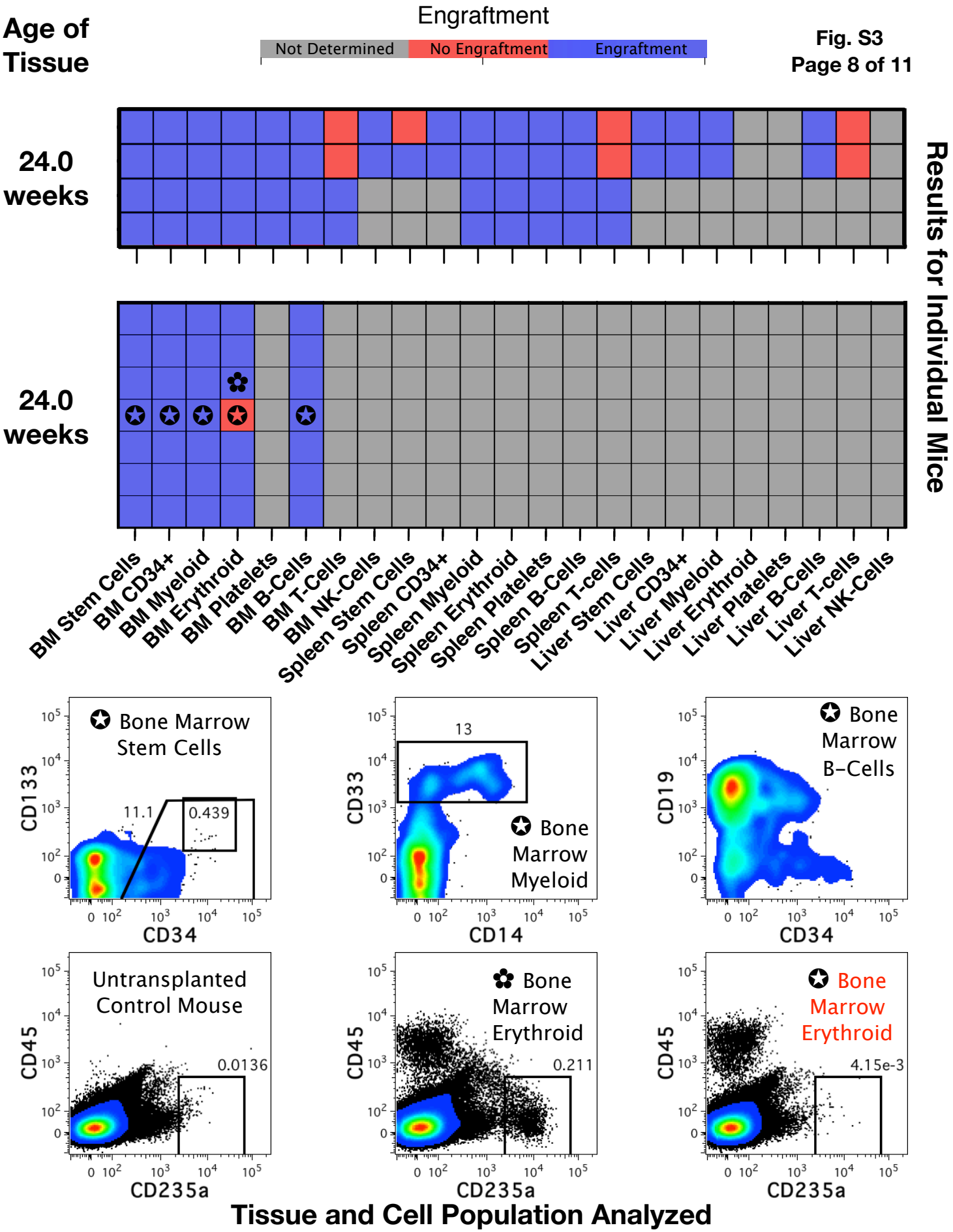

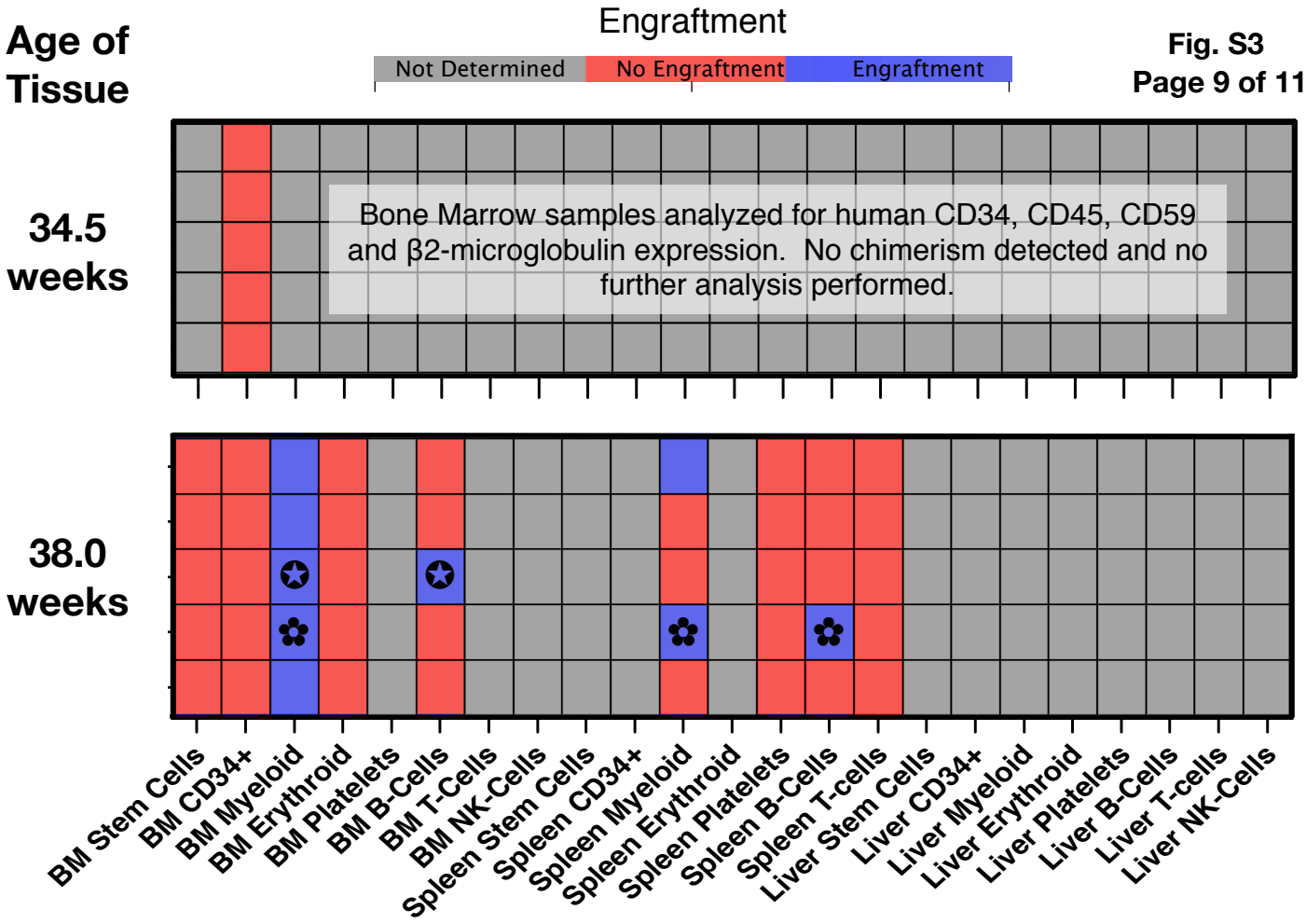

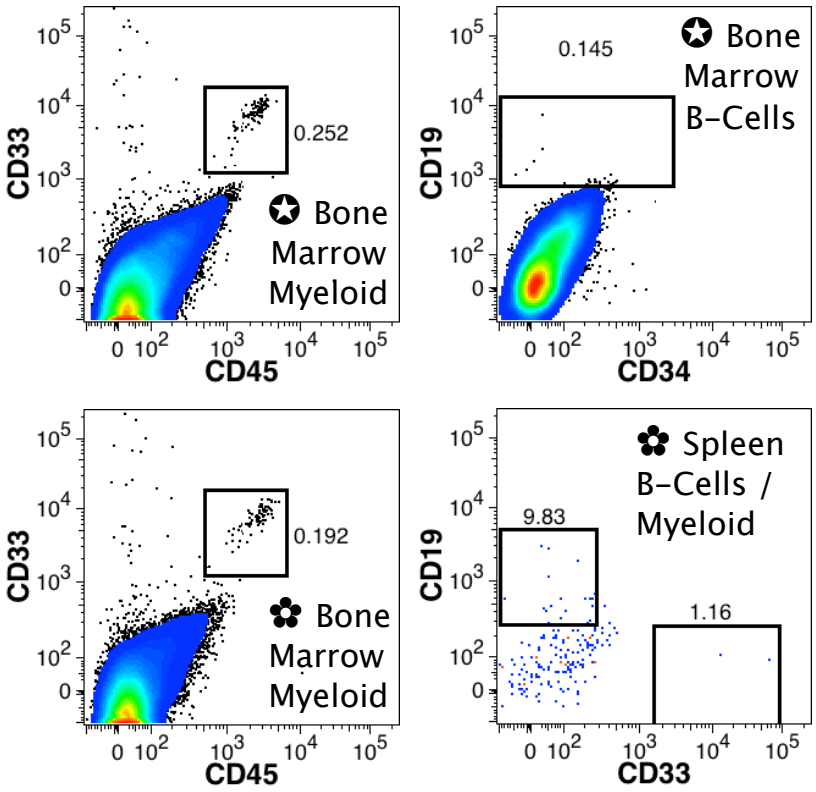

Tissue and Cell Population Analyzed

Results for Individual Mice

Age of Tissue

Engraftment

Not Determined | No Engraftment | Engraftment

38.4 weeks

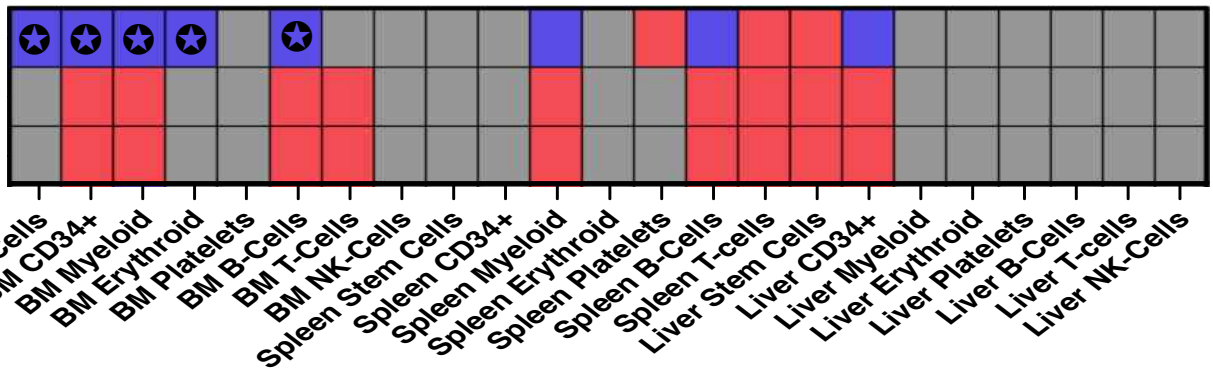

BM Stem Cells
BM CD34+
BM Myeloid
BM Erythroid
BM Platelets
BM B-Cells
BM T-Cells
BM NK-Cells
Spleen Stem Cells
Spleen CD34+
Spleen Myeloid
Spleen Erythroid
Spleen Platelets
Spleen B-Cells
Spleen T-cells
Liver Stem Cells
Liver CD34+
Liver Myeloid
Liver Erythroid
Liver Platelets
Liver B-Cells
Liver T-cells
Liver NK-Cells

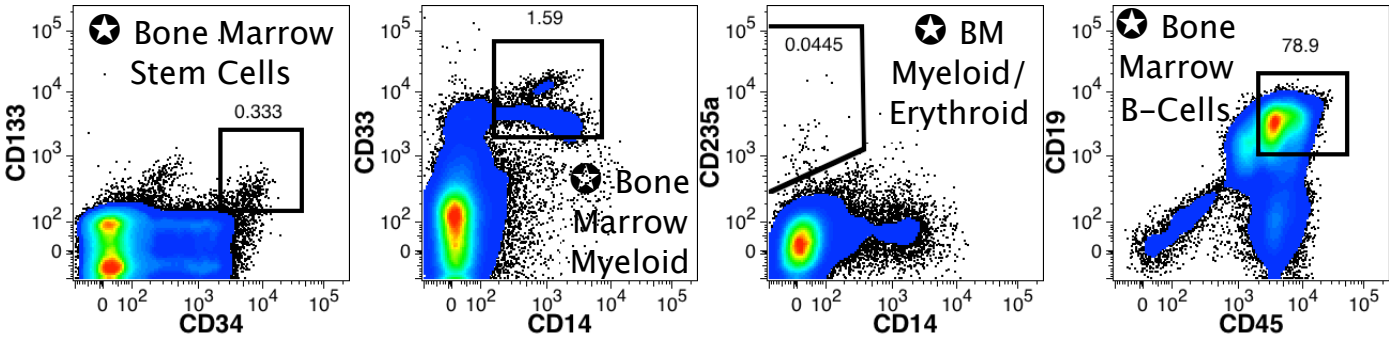

39.0 weeks

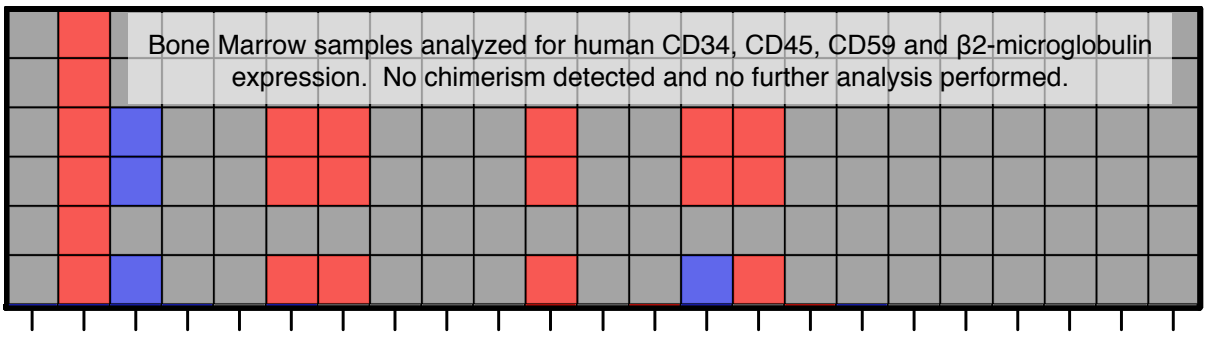

Bone Marrow samples analyzed for human CD34, CD45, CD59 and β2-microglobulin expression. No chimerism detected and no further analysis performed.

39.0 weeks

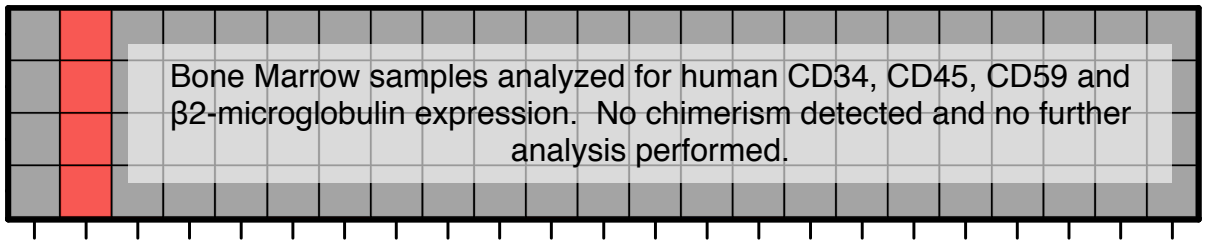

Bone Marrow samples analyzed for human CD34, CD45, CD59 and β2-microglobulin expression. No chimerism detected and no further analysis performed.

BM Stem Cells
BM CD34+
BM Myeloid
BM Erythroid
BM Platelets
BM B-Cells
BM T-Cells
BM NK-Cells
Spleen Stem Cells
Spleen CD34+
Spleen Myeloid
Spleen Erythroid
Spleen Platelets
Spleen B-Cells
Spleen T-cells
Liver Stem Cells
Liver CD34+
Liver Myeloid
Liver Erythroid
Liver Platelets
Liver B-Cells
Liver T-cells
Liver NK-Cells

Tissue and Cell Population Analyzed

Results for Individual Mice

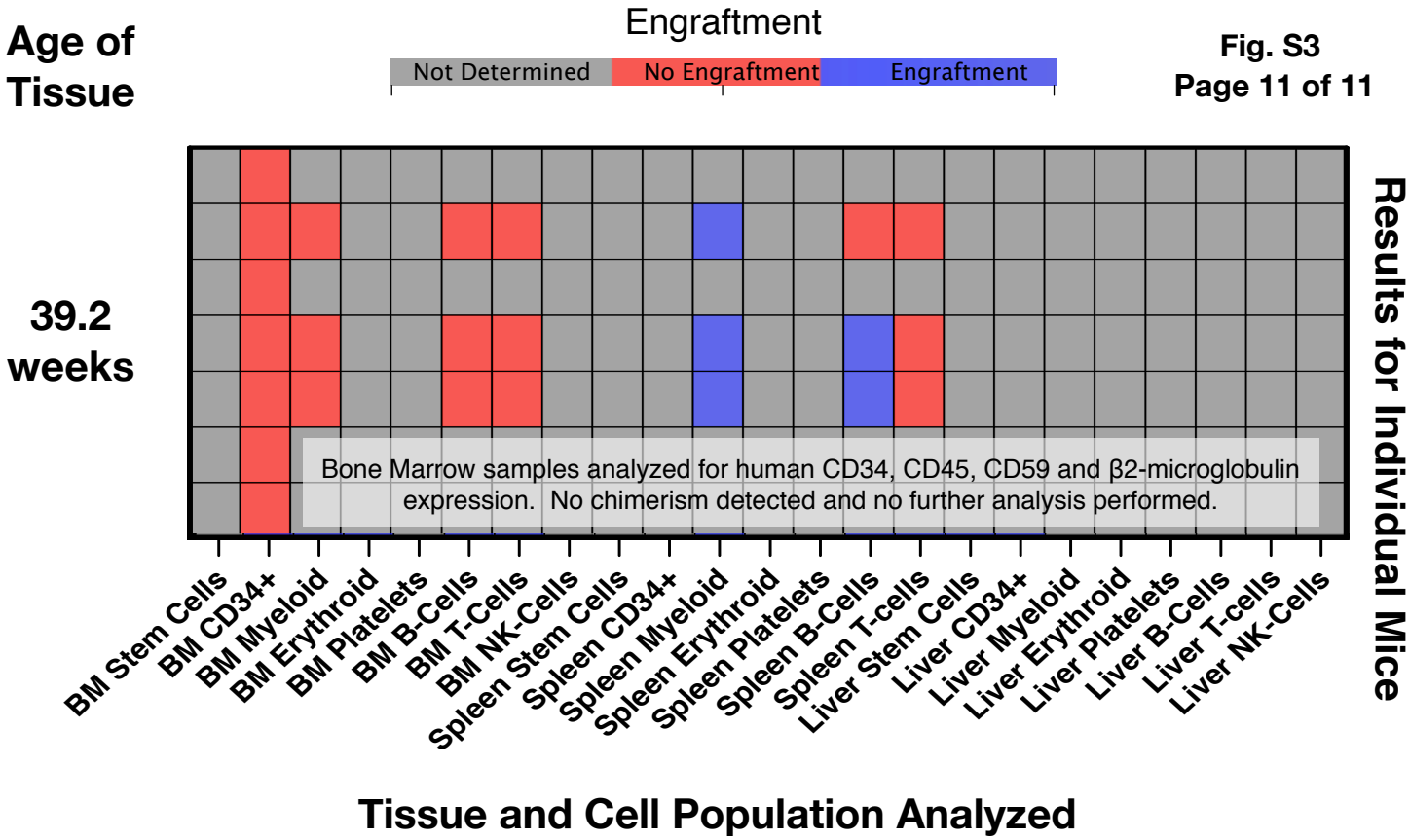

Fig. S3. Overview of hematopoietic engraftment and selected flow cytometric analyses of chorion transplants in immunodeficient mice. Heat maps indicate the lineage analyses performed for the three hematopoietic tissues examined and whether engraftment was observed for each of the 28 transplanted cell isolates. Results are presented according to gestation age of the donor tissue (youngest at the top), which parallels the presentation of the summary findings presented in Fig. 5B of the manuscript. Each row of a heat map represents a single transplanted mouse. At a minimum, all mice were analyzed with a single panel of antibodies staining widely expressed human antigens (CD34, CD45, CD59 and CD81 or β2-microglobulin). If no human chimerism was detected, then no further analysis was performed. Otherwise, mice were analyzed for the presence of human CD34+, myeloid, erythroid and B-lymphoid bone marrow cells in addition to any other indicated tissue/lineage analyses. Fig. 6 in the manuscript presents a broad analysis of hematopoietic engraftment in one mouse. Additional examples of flow cytometry results showing full and partial engraftment are presented herein: 1) First trimester tissues generally did not engraft mice with the exception of T- and B-lymphocyte engraftment observed in some mice (6.2 and 11.3 weeks' gestation grafts), 2) the youngest tissue yielding full engraftment was 15.2 weeks' gestation, 3) another examples of full engraftment is shown for the 17.3 weeks' gestation graft, 4) an example of partial (B-cell) engraftment is shown for the 20.1 weeks' gestation sample, 5) anther example of partial engraftment in which erythroid engraftment could not be documented is shown for one of the 24.0 weeks' gestation samples, 6) partial myeloid engraftment was observed in some transplants of third trimester tissues - e.g, 38.0 weeks' gestation- with very low numbers of CD19+ cells being observed as well, in some cases, and 7) a single case of full engraftment was observed in a mouse transplanted with third trimester cells (38.4 weeks' gestation). The symbols ✪ and ✿ are used to indicate the mouse, tissue and cell lineage represented by the flow cytometry data shown associated with the individual heat maps. Analyses labeled with red text represent negative data and black text represents positive engraftment data.

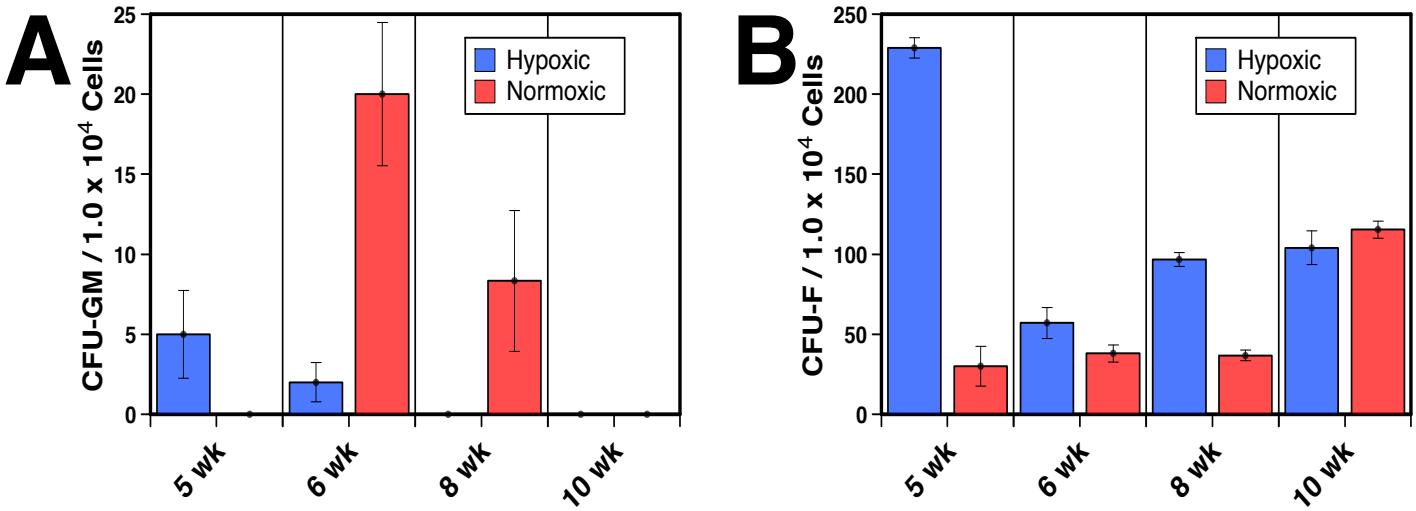

Supplemental Figure S4. Oxygen levels do not significantly affect the in vitro hematopoietic potential of 1st trimester chorionic hematopoietic progenitors. Prior to 7 wks the chorion and the chorionic villi could not be separated and were analyzed together. Afterwards the chorion was processed separately from the villi. Cells were cultured for 3 wks in either physiological hypoxia (1% O_2, blue) or standard conditions (20% O_2, red). (A) CFU-GM (granulocyte-macrophage) colonies were enumerated at the gestational ages indicated. (B) CFU-F (fibroblast) colonies in the same cultures were also enumerated. Data in A and B are mean ± SEM of 3-5 plates/ sample.

Supplementary Table S1. This table contains a full list of the monoclonal antibodies against human and mouse antigens utilized in flow cytometry analyses, including the fluorochrome label, isotype, clone name and source.

Click here to Download Table S1